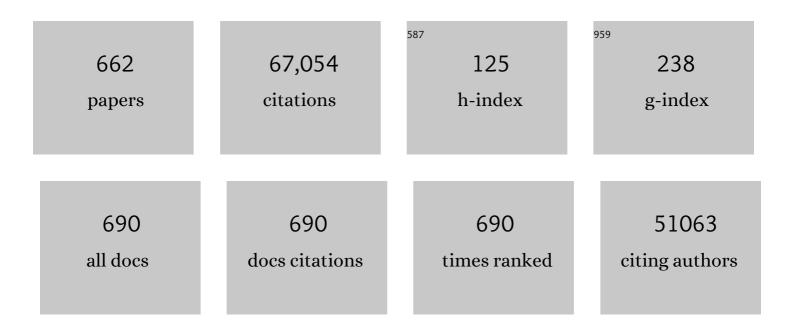
List of Publications by Year in descending order

Source: https://exaly.com/author-pdf/2708916/publications.pdf Version: 2024-02-01



Ι ι-Ιι ινι λλ/ανι

#	Article	IF	CITATIONS
1	Lithium–Sulfur Batteries: Electrochemistry, Materials, and Prospects. Angewandte Chemie - International Edition, 2013, 52, 13186-13200.	7.2	2,329
2	Nanostructured Materials for Electrochemical Energy Conversion and Storage Devices. Advanced Materials, 2008, 20, 2878-2887.	11.1	2,054
3	Understanding the High Activity of Fe–N–C Electrocatalysts in Oxygen Reduction: Fe/Fe ₃ C Nanoparticles Boost the Activity of Fe–N _{<i>x</i>} . Journal of the American Chemical Society, 2016, 138, 3570-3578.	6.6	1,549
4	Self-Assembled 3D Flowerlike Iron Oxide Nanostructures and Their Application in Water Treatment. Advanced Materials, 2006, 18, 2426-2431.	11.1	1,526
5	Smaller Sulfur Molecules Promise Better Lithium–Sulfur Batteries. Journal of the American Chemical Society, 2012, 134, 18510-18513.	6.6	1,499
6	Carbon Coated Fe ₃ O ₄ Nanospindles as a Superior Anode Material for Lithiumâ€ion Batteries. Advanced Functional Materials, 2008, 18, 3941-3946.	7.8	1,177
7	Binding SnO ₂ Nanocrystals in Nitrogenâ€Doped Graphene Sheets as Anode Materials for Lithiumâ€ion Batteries. Advanced Materials, 2013, 25, 2152-2157.	11.1	1,089
8	Cobalt in Nitrogen-Doped Graphene as Single-Atom Catalyst for High-Sulfur Content Lithium–Sulfur Batteries. Journal of the American Chemical Society, 2019, 141, 3977-3985.	6.6	1,071
9	Tinâ€Nanoparticles Encapsulated in Elastic Hollow Carbon Spheres for Highâ€Performance Anode Material in Lithiumâ€Ion Batteries. Advanced Materials, 2008, 20, 1160-1165.	11.1	1,002
10	Self-Assembled Vanadium Pentoxide (V2O5) Hollow Microspheres from Nanorods and Their Application in Lithium-Ion Batteries. Angewandte Chemie - International Edition, 2005, 44, 4391-4395.	7.2	840
11	Acute toxicological effects of copper nanoparticles in vivo. Toxicology Letters, 2006, 163, 109-120.	0.4	825
12	Electronic and Morphological Dual Modulation of Cobalt Carbonate Hydroxides by Mn Doping toward Highly Efficient and Stable Bifunctional Electrocatalysts for Overall Water Splitting. Journal of the American Chemical Society, 2017, 139, 8320-8328.	6.6	745
13	Pt Hollow Nanospheres: Facile Synthesis and Enhanced Electrocatalysts. Angewandte Chemie - International Edition, 2004, 43, 1540-1543.	7.2	662
14	LiFePO ₄ Nanoparticles Embedded in a Nanoporous Carbon Matrix: Superior Cathode Material for Electrochemical Energy‣torage Devices. Advanced Materials, 2009, 21, 2710-2714.	11.1	647
15	Spaceâ€Confinementâ€Induced Synthesis of Pyridinic―and Pyrrolicâ€Nitrogenâ€Doped Graphene for the Catalysis of Oxygen Reduction. Angewandte Chemie - International Edition, 2013, 52, 11755-11759.	7.2	620
16	Rutile-TiO ₂ Nanocoating for a High-Rate Li ₄ Ti ₅ O ₁₂ Anode of a Lithium-Ion Battery. Journal of the American Chemical Society, 2012, 134, 7874-7879.	6.6	602
17	Cascade anchoring strategy for general mass production of high-loading single-atomic metal-nitrogen catalysts. Nature Communications, 2019, 10, 1278.	5.8	591
18	A Flexible Solid Electrolyte Interphase Layer for Long‣ife Lithium Metal Anodes. Angewandte Chemie - International Edition, 2018, 57, 1505-1509.	7.2	590

#	Article	IF	CITATIONS
19	Pomegranate-like N,P-Doped Mo ₂ C@C Nanospheres as Highly Active Electrocatalysts for Alkaline Hydrogen Evolution. ACS Nano, 2016, 10, 8851-8860.	7.3	575
20	Synthesis of Hierarchically Structured Metal Oxides and their Application in Heavy Metal Ion Removal. Advanced Materials, 2008, 20, 2977-2982.	11.1	568
21	Mass Production and High Photocatalytic Activity of ZnS Nanoporous Nanoparticles. Angewandte Chemie - International Edition, 2005, 44, 1269-1273.	7.2	558
22	Zn–Cu–In–Se Quantum Dot Solar Cells with a Certified Power Conversion Efficiency of 11.6%. Journal of the American Chemical Society, 2016, 138, 4201-4209.	6.6	537
23	Nanocarbon Networks for Advanced Rechargeable Lithium Batteries. Accounts of Chemical Research, 2012, 45, 1759-1769.	7.6	533
24	A Highâ€Energy Roomâ€Temperature Sodiumâ€Sulfur Battery. Advanced Materials, 2014, 26, 1261-1265.	11.1	525
25	Watermelonâ€Inspired Si/C Microspheres with Hierarchical Buffer Structures for Densely Compacted Lithiumâ€Ion Battery Anodes. Advanced Energy Materials, 2017, 7, 1601481.	10.2	508
26	Se-Doping Activates FeOOH for Cost-Effective and Efficient Electrochemical Water Oxidation. Journal of the American Chemical Society, 2019, 141, 7005-7013.	6.6	460
27	Controllable Pt Nanoparticle Deposition on Carbon Nanotubes as an Anode Catalyst for Direct Methanol Fuel Cells. Journal of Physical Chemistry B, 2005, 109, 22212-22216.	1.2	454
28	Selfâ€Assembled Nanocomposite of Silicon Nanoparticles Encapsulated in Graphene through Electrostatic Attraction for Lithiumâ€ion Batteries. Advanced Energy Materials, 2012, 2, 1086-1090.	10.2	447
29	Suppressing the P2–O2 Phase Transition of Na _{0.67} Mn _{0.67} Ni _{0.33} O ₂ by Magnesium Substitution for Improved Sodiumâ€Ion Batteries. Angewandte Chemie - International Edition, 2016, 55, 7445-7449.	7.2	439
30	Selfâ€Templated Fabrication of MoNi ₄ /MoO _{3â€} <i>_x</i> Nanorod Arrays with Dual Active Components for Highly Efficient Hydrogen Evolution. Advanced Materials, 2017, 29, 1703311.	11.1	437
31	Improving the Electrode Performance of Ge through Ge@C Core–Shell Nanoparticles and Graphene Networks. Journal of the American Chemical Society, 2012, 134, 2512-2515.	6.6	436
32	3D Flowerlike Ceria Micro/Nanocomposite Structure and Its Application for Water Treatment and CO Removal. Chemistry of Materials, 2007, 19, 1648-1655.	3.2	433
33	Nanostructured Polyaniline-Decorated Pt/C@PANI Core–Shell Catalyst with Enhanced Durability and Activity. Journal of the American Chemical Society, 2012, 134, 13252-13255.	6.6	430
34	MoS ₂ /CdS Nanosheets-on-Nanorod Heterostructure for Highly Efficient Photocatalytic H ₂ Generation under Visible Light Irradiation. ACS Applied Materials & Interfaces, 2016, 8, 15258-15266.	4.0	426
35	Facile synthesis of silicon nanoparticles inserted into graphene sheets as improved anode materials for lithium-ion batteries. Chemical Communications, 2012, 48, 2198.	2.2	417
36	Stable Li Plating/Stripping Electrochemistry Realized by a Hybrid Li Reservoir in Spherical Carbon Granules with 3D Conducting Skeletons. Journal of the American Chemical Society, 2017, 139, 5916-5922.	6.6	410

#	Article	IF	CITATIONS
37	Subzeroâ€Temperature Cathode for a Sodiumâ€ŀon Battery. Advanced Materials, 2016, 28, 7243-7248.	11.1	406
38	Dendrite-Free Li-Metal Battery Enabled by a Thin Asymmetric Solid Electrolyte with Engineered Layers. Journal of the American Chemical Society, 2018, 140, 82-85.	6.6	404
39	Uniform Lithium Nucleation/Growth Induced by Lightweight Nitrogenâ€Đoped Graphitic Carbon Foams for Highâ€Performance Lithium Metal Anodes. Advanced Materials, 2018, 30, 1706216.	11.1	401
40	Reshaping Lithium Plating/Stripping Behavior via Bifunctional Polymer Electrolyte for Room-Temperature Solid Li Metal Batteries. Journal of the American Chemical Society, 2016, 138, 15825-15828.	6.6	399
41	Sulfur Encapsulated in Graphitic Carbon Nanocages for Highâ€Rate and Longâ€Cycle Lithium–Sulfur Batteries. Advanced Materials, 2016, 28, 9539-9544.	11.1	392
42	On-Surface Synthesis of Single-Layered Two-Dimensional Covalent Organic Frameworks via Solid–Vapor Interface Reactions. Journal of the American Chemical Society, 2013, 135, 10470-10474.	6.6	370
43	A Sandwichâ€Like Hierarchically Porous Carbon/Graphene Composite as a Highâ€Performance Anode Material for Sodiumâ€Ion Batteries. Advanced Energy Materials, 2014, 4, 1301584.	10.2	365
44	Mono dispersed SnO2 nanoparticles on both sides of single layer graphene sheets as anode materials in Li-ion batteries. Journal of Materials Chemistry, 2010, 20, 5462.	6.7	362
45	Carbonâ€Nanotubeâ€Decorated Nanoâ€LiFePO ₄ @C Cathode Material with Superior Highâ€Rate and Lowâ€Temperature Performances for Lithiumâ€Ion Batteries. Advanced Energy Materials, 2013, 3, 1155-1160.	10.2	351
46	Hierarchically Structured Cobalt Oxide (Co3O4):Â The Morphology Control and Its Potential in Sensors. Journal of Physical Chemistry B, 2006, 110, 15858-15863.	1.2	339
47	Highâ€Capacity Cathode Material with High Voltage for Liâ€lon Batteries. Advanced Materials, 2018, 30, 1705575.	11.1	333
48	Extended Electrochemical Window of Solid Electrolytes via Heterogeneous Multilayered Structure for Highâ€Voltage Lithium Metal Batteries. Advanced Materials, 2019, 31, e1807789.	11.1	333
49	Free-Standing Hollow Carbon Fibers as High-Capacity Containers for Stable Lithium Metal Anodes. Joule, 2017, 1, 563-575.	11.7	329
50	Highly Dispersed RuO ₂ Nanoparticles on Carbon Nanotubes: Facile Synthesis and Enhanced Supercapacitance Performance. Journal of Physical Chemistry C, 2010, 114, 2448-2451.	1.5	312
51	A Roomâ€Temperature Reactiveâ€Template Route to Mesoporous ZnGa ₂ O ₄ with Improved Photocatalytic Activity in Reduction of CO ₂ . Angewandte Chemie - International Edition, 2010, 49, 6400-6404.	7.2	307
52	Designing Air-Stable O3-Type Cathode Materials by Combined Structure Modulation for Na-Ion Batteries. Journal of the American Chemical Society, 2017, 139, 8440-8443.	6.6	303
53	Three-Dimensional Self-Organization of Supramolecular Self-Assembled Porphyrin Hollow Hexagonal Nanoprisms. Journal of the American Chemical Society, 2005, 127, 17090-17095.	6.6	302
54	Gold Hollow Nanospheres:Â Tunable Surface Plasmon Resonance Controlled by Interior-Cavity Sizes. Journal of Physical Chemistry B, 2005, 109, 7795-7800.	1.2	301

#	Article	IF	CITATIONS
55	Synthesis of MoS2 nanosheet–graphene nanosheet hybrid materials for stable lithium storage. Chemical Communications, 2013, 49, 1838.	2.2	293
56	Cu‣i Nanocable Arrays as Highâ€Rate Anode Materials for Lithiumâ€Ion Batteries. Advanced Materials, 2011, 23, 4415-4420.	11.1	283
57	Ionothermal synthesis of sulfur-doped porous carbons hybridized with graphene as superior anode materials for lithium-ion batteries. Chemical Communications, 2012, 48, 10663.	2.2	278
58	Research progress regarding Si-based anode materials towards practical application in high energy density Li-ion batteries. Materials Chemistry Frontiers, 2017, 1, 1691-1708.	3.2	277
59	Degradation Chemistry and Stabilization of Exfoliated Few-Layer Black Phosphorus in Water. Journal of the American Chemical Society, 2018, 140, 7561-7567.	6.6	273
60	Engineering Janus Interfaces of Ceramic Electrolyte via Distinct Functional Polymers for Stable High-Voltage Li-Metal Batteries. Journal of the American Chemical Society, 2019, 141, 9165-9169.	6.6	272
61	Crystallinityâ€Modulated Electrocatalytic Activity of a Nickel(II) Borate Thin Layer on Ni ₃ B for Efficient Water Oxidation. Angewandte Chemie - International Edition, 2017, 56, 6572-6577.	7.2	271
62	Introducing Dual Functional CNT Networks into CuO Nanomicrospheres toward Superior Electrode Materials for Lithium-Ion Batteries. Chemistry of Materials, 2008, 20, 3617-3622.	3.2	270
63	Molecular Orientation and Ordered Structure of Benzenethiol Adsorbed on Gold(111). Journal of Physical Chemistry B, 2000, 104, 3563-3569.	1.2	266
64	Controlling the Compositional Chemistry in Single Nanoparticles for Functional Hollow Carbon Nanospheres. Journal of the American Chemical Society, 2017, 139, 13492-13498.	6.6	264
65	Engineering Hollow Carbon Architecture for High-Performance K-Ion Battery Anode. Journal of the American Chemical Society, 2018, 140, 7127-7134.	6.6	255
66	Insight into the Effect of Oxygen Vacancy Concentration on the Catalytic Performance of MnO ₂ . ACS Catalysis, 2015, 5, 4825-4832.	5.5	244
67	Synthesis of Monodispersed Wurtzite Structure CuInSe ₂ Nanocrystals and Their Application in High-Performance Organicâ l'norganic Hybrid Photodetectors. Journal of the American Chemical Society, 2010, 132, 12218-12221.	6.6	242
68	Superior radical polymer cathode material with a two-electron process redox reaction promoted by graphene. Energy and Environmental Science, 2012, 5, 5221-5225.	15.6	241
69	Facile synthesis of MoS2@CMK-3 nanocomposite as an improved anode material for lithium-ion batteries. Nanoscale, 2012, 4, 5868.	2.8	240
70	GeSe Thin-Film Solar Cells Fabricated by Self-Regulated Rapid Thermal Sublimation. Journal of the American Chemical Society, 2017, 139, 958-965.	6.6	238
71	Confined Synthesis of Two-Dimensional Covalent Organic Framework Thin Films within Superspreading Water Layer. Journal of the American Chemical Society, 2018, 140, 12152-12158.	6.6	231
72	Anisotropic Photoresponse Properties of Single Micrometerâ€Sized GeSe Nanosheet. Advanced Materials, 2012, 24, 4528-4533.	11.1	229

#	Article	IF	CITATIONS
73	In-situ plasticized polymer electrolyte with double-network for flexible solid-state lithium-metal batteries. Energy Storage Materials, 2018, 10, 85-91.	9.5	227
74	Polar Solvent Induced Lattice Distortion of Cubic CsPbI ₃ Nanocubes and Hierarchical Self-Assembly into Orthorhombic Single-Crystalline Nanowires. Journal of the American Chemical Society, 2018, 140, 11705-11715.	6.6	223
75	Embedding Pt Nanocrystals in N-Doped Porous Carbon/Carbon Nanotubes toward Highly Stable Electrocatalysts for the Oxygen Reduction Reaction. ACS Catalysis, 2015, 5, 2903-2909.	5.5	221
76	Recent developments in electrode materials for potassium-ion batteries. Journal of Materials Chemistry A, 2019, 7, 4334-4352.	5.2	214
77	Fabricating and Controlling Molecular Self-Organization at Solid Surfaces:  Studies by Scanning Tunneling Microscopy. Accounts of Chemical Research, 2006, 39, 334-342.	7.6	211
78	Electrochemical (De)Lithiation of 1D Sulfur Chains in Li–S Batteries: A Model System Study. Journal of the American Chemical Society, 2015, 137, 2215-2218.	6.6	209
79	α-Fe ₂ O ₃ Nanostructures: Inorganic Salt-Controlled Synthesis and Their Electrochemical Performance toward Lithium Storage. Journal of Physical Chemistry C, 2008, 112, 16824-16829.	1.5	206
80	General Space-Confined On-Substrate Fabrication of Thickness-Adjustable Hybrid Perovskite Single-Crystalline Thin Films. Journal of the American Chemical Society, 2016, 138, 16196-16199.	6.6	205
81	Electrochemical Sensor for Detecting Ultratrace Nitroaromatic Compounds Using Mesoporous SiO2-Modified Electrode. Analytical Chemistry, 2006, 78, 1967-1971.	3.2	204
82	Grapheneâ€Like Singleâ€Layered Covalent Organic Frameworks: Synthesis Strategies and Application Prospects. Advanced Materials, 2014, 26, 6912-6920.	11.1	200
83	Solid–Solution-Based Metal Alloy Phase for Highly Reversible Lithium Metal Anode. Journal of the American Chemical Society, 2020, 142, 8818-8826.	6.6	199
84	Mitigating Voltage Decay of Li-Rich Cathode Material via Increasing Ni Content for Lithium-Ion Batteries. ACS Applied Materials & Interfaces, 2016, 8, 20138-20146.	4.0	197
85	Atomic Structure of Adsorbed Sulfate on Rh(111) in Sulfuric Acid Solution. The Journal of Physical Chemistry, 1995, 99, 9507-9513.	2.9	193
86	Symbiotic Coaxial Nanocables: Facile Synthesis and an Efficient and Elegant Morphological Solution to the Lithium Storage Problem. Chemistry of Materials, 2010, 22, 1908-1914.	3.2	193
87	Mitigating Interfacial Potential Drop of Cathode–Solid Electrolyte via Ionic Conductor Layer To Enhance Interface Dynamics for Solid Batteries. Journal of the American Chemical Society, 2018, 140, 6767-6770.	6.6	192
88	Steering elementary steps towards efficient alkaline hydrogen evolution via size-dependent Ni/NiO nanoscale heterosurfaces. National Science Review, 2020, 7, 27-36.	4.6	192
89	Construction and repair of highly ordered 2D covalent networks by chemical equilibrium regulation. Chemical Communications, 2012, 48, 2943.	2.2	188
90	Synergism of Al-containing solid electrolyte interphase layer and Al-based colloidal particles for stable lithium anode. Nano Energy, 2017, 36, 411-417.	8.2	187

#	Article	IF	CITATIONS
91	SnO ₂ -Based Hierarchical Nanomicrostructures: Facile Synthesis and Their Applications in Gas Sensors and Lithium-Ion Batteries. Journal of Physical Chemistry C, 2009, 113, 14213-14219.	1.5	183
92	Rational Design of Anode Materials Based on Groupâ€IVA Elements (Si, Ge, and Sn) for Lithiumâ€lon Batteries. Chemistry - an Asian Journal, 2013, 8, 1948-1958.	1.7	181
93	Air-Stable In-Plane Anisotropic GeSe ₂ for Highly Polarization-Sensitive Photodetection in Short Wave Region. Journal of the American Chemical Society, 2018, 140, 4150-4156.	6.6	180
94	Characterization of surface property of poly(lactide-co-glycolide) after oxygen plasma treatment. Biomaterials, 2004, 25, 4777-4783.	5.7	178
95	Electrospray Synthesis of Silicon/Carbon Nanoporous Microspheres as Improved Anode Materials for Lithium-Ion Batteries. Journal of Physical Chemistry C, 2011, 115, 14148-14154.	1.5	177
96	Template-Induced Inclusion Structures with Copper(II) Phthalocyanine and Coronene as Guests in Two-Dimensional Hydrogen-Bonded Host Networks. Journal of Physical Chemistry B, 2004, 108, 5161-5165.	1.2	173
97	Microscopic Investigation of Grain Boundaries in Organolead Halide Perovskite Solar Cells. ACS Applied Materials & Interfaces, 2015, 7, 28518-28523.	4.0	173
98	Surface Confined Metallosupramolecular Architectures: Formation and Scanning Tunneling Microscopy Characterization. Accounts of Chemical Research, 2009, 42, 249-259.	7.6	172
99	Robust Expandable Carbon Nanotube Scaffold for Ultrahigh apacity Lithiumâ€Metal Anodes. Advanced Materials, 2018, 30, e1800884.	11.1	171
100	Electrospun Silicon Nanoparticle/Porous Carbon Hybrid Nanofibers for Lithiumâ€lon Batteries. Small, 2013, 9, 2684-2688.	5.2	164
101	Biodegradable, Hydrogen Peroxide, and Glutathione Dual Responsive Nanoparticles for Potential Programmable Paclitaxel Release. Journal of the American Chemical Society, 2018, 140, 7373-7376.	6.6	161
102	Oriented Covalent Organic Framework Film on Graphene for Robust Ambipolar Vertical Organic Field-Effect Transistor. Chemistry of Materials, 2017, 29, 4367-4374.	3.2	160
103	The 2021 battery technology roadmap. Journal Physics D: Applied Physics, 2021, 54, 183001.	1.3	158
104	In-Situ Loading of Noble Metal Nanoparticles on Hydroxyl-Group-Rich Titania Precursor and Their Catalytic Applications. Chemistry of Materials, 2007, 19, 4557-4562.	3.2	156
105	Antioxidative function and biodistribution of [Gd@C82(OH)22]n nanoparticles in tumor-bearing mice. Biochemical Pharmacology, 2006, 71, 872-881.	2.0	152
106	Direct Evidence of Molecular Aggregation and Degradation Mechanism of Organic Light-Emitting Diodes under Joule Heating:Â an STM and Photoluminescence Study. Journal of Physical Chemistry B, 2005, 109, 1675-1682.	1.2	151
107	Core–shell structured TiO ₂ @polydopamine for highly active visible-light photocatalysis. Chemical Communications, 2016, 52, 7122-7125.	2.2	151
108	Oriented Two-Dimensional Covalent Organic Framework Films for Near-Infrared Electrochromic Application. Journal of the American Chemical Society, 2019, 141, 19831-19838.	6.6	151

#	Article	IF	CITATIONS
109	Metastable Rock Salt Oxide-Mediated Synthesis of High-Density Dual-Protected M@NC for Long-Life Rechargeable Zinc–Air Batteries with Record Power Density. Journal of the American Chemical Society, 2020, 142, 7116-7127.	6.6	147
110	Facile synthesis of nanoporous anatase spheres and their environmental applications. Chemical Communications, 2008, , 1184.	2.2	146
111	Bridging Interparticle Li ⁺ Conduction in a Soft Ceramic Oxide Electrolyte. Journal of the American Chemical Society, 2021, 143, 5717-5726.	6.6	144
112	Well-dispersed bi-component-active CoO/CoFe ₂ O ₄ nanocomposites with tunable performances as anode materials for lithium-ion batteries. Chemical Communications, 2012, 48, 410-412.	2.2	141
113	Rational design and electron transfer kinetics of MoS2/CdS nanodots-on-nanorods for efficient visible-light-driven hydrogen generation. Nano Energy, 2016, 28, 319-329.	8.2	140
114	Direct tracking of the polysulfide shuttling and interfacial evolution in all-solid-state lithium–sulfur batteries: a degradation mechanism study. Energy and Environmental Science, 2019, 12, 2496-2506.	15.6	140
115	Uniform Nucleation of Lithium in 3D Current Collectors via Bromide Intermediates for Stable Cycling Lithium Metal Batteries. Journal of the American Chemical Society, 2018, 140, 18051-18057.	6.6	138
116	Photoacoustic Imaging Guided Nearâ€Infrared Photothermal Therapy Using Highly Waterâ€Dispersible Singleâ€Walled Carbon Nanohorns as Theranostic Agents. Advanced Functional Materials, 2014, 24, 6621-6628.	7.8	137
117	Efficient 3D Conducting Networks Built by Graphene Sheets and Carbon Nanoparticles for High-Performance Silicon Anode. ACS Applied Materials & Interfaces, 2012, 4, 2824-2828.	4.0	135
118	Infrared Absorption Enhancement for CO Adsorbed on Au Films in Perchloric Acid Solutions and Effects of Surface Structure Studied by Cyclic Voltammetry, Scanning Tunneling Microscopy, and Surface-Enhanced IR Spectroscopy. Journal of Physical Chemistry B, 1999, 103, 2460-2466.	1.2	133
119	Orientational Phase Transition in a Pyridine Adlayer on Gold(111) in Aqueous Solution Studied by in Situ Infrared Spectroscopy and Scanning Tunneling Microscopy. Langmuir, 1998, 14, 6992-6998.	1.6	131
120	A robust composite of SnO2 hollow nanospheres enwrapped by graphene as a high-capacity anode material for lithium-ion batteries. Journal of Materials Chemistry, 2012, 22, 17456.	6.7	129
121	Building an Air Stable and Lithium Deposition Regulable Garnet Interface from Moderateâ€Temperature Conversion Chemistry. Angewandte Chemie - International Edition, 2020, 59, 12069-12075.	7.2	128
122	In Situ One-Step Method for Preparing Carbon Nanotubes and Pt Composite Catalysts and Their Performance for Methanol Oxidation. Journal of Physical Chemistry C, 2007, 111, 11174-11179.	1.5	127
123	High-safety lithium-sulfur battery with prelithiated Si/C anode and ionic liquid electrolyte. Electrochimica Acta, 2013, 91, 58-61.	2.6	127
124	A Twoâ€Dimensional Holeâ€Transporting Material for Highâ€Performance Perovskite Solar Cells with 20 % Average Efficiency. Angewandte Chemie - International Edition, 2018, 57, 10959-10965.	7.2	127
125	Interfacial Mechanism in Lithium–Sulfur Batteries: How Salts Mediate the Structure Evolution and Dynamics. Journal of the American Chemical Society, 2018, 140, 8147-8155.	6.6	125
126	Surface Stabilized Porphyrin and Phthalocyanine Two-Dimensional Network Connected by Hydrogen Bonds. Journal of Physical Chemistry B, 2001, 105, 10838-10841.	1.2	122

#	Article	IF	CITATIONS
127	Hierarchical Nanowire Arrays as Three-Dimensional Fractal Nanobiointerfaces for High Efficient Capture of Cancer Cells. Nano Letters, 2016, 16, 766-772.	4.5	122
128	Controllable AuPt bimetallic hollow nanostructures. Chemical Communications, 2004, , 1496.	2.2	121
129	Structural Engineering of Multishelled Hollow Carbon Nanostructures for Highâ€Performance Naâ€Ion Battery Anode. Advanced Energy Materials, 2018, 8, 1800855.	10.2	121
130	Better lithium-ion batteries with nanocable-like electrode materials. Energy and Environmental Science, 2011, 4, 1634.	15.6	119
131	Globally homochiral assembly of two-dimensional molecular networks triggered by co-absorbers. Nature Communications, 2013, 4, 1389.	5.8	119
132	Insight into the Interfacial Process and Mechanism in Lithium–Sulfur Batteries: An In Situ AFM Study. Angewandte Chemie - International Edition, 2016, 55, 15835-15839.	7.2	119
133	ITO@Cu ₂ S Tunnel Junction Nanowire Arrays as Efficient Counter Electrode for Quantum-Dot-Sensitized Solar Cells. Nano Letters, 2014, 14, 365-372.	4.5	118
134	Spin-coated silicon nanoparticle/graphene electrode as a binder-free anode for high-performance lithium-ion batteries. Nano Research, 2012, 5, 845-853.	5.8	117
135	Formation of Halogen Bond-Based 2D Supramolecular Assemblies by Electric Manipulation. Journal of the American Chemical Society, 2015, 137, 6128-6131.	6.6	117
136	Wurtzite Cu2ZnSnSe4 nanocrystals for high-performance organic–inorganic hybrid photodetectors. NPG Asia Materials, 2012, 4, e2-e2.	3.8	116
137	In situ scanning tunneling microscopy of adsorbed sulfate on well-defined Pd(111) in sulfuric acid solution. Journal of Electroanalytical Chemistry, 2000, 484, 189-193.	1.9	115
138	Insights into the Mechanism of Methanol-to-Olefin Conversion at Zeolites with Systematically Selected Framework Structures. Angewandte Chemie - International Edition, 2006, 45, 6512-6515.	7.2	115
139	Room Temperature Ionic Liquids Assisted Green Synthesis of Nanocrystalline Porous SnO ₂ and Their Gas Sensor Behaviors. Crystal Growth and Design, 2008, 8, 4165-4172.	1.4	114
140	Ordered Niâ^'Cu Nanowire Array with Enhanced Coercivity. Chemistry of Materials, 2003, 15, 664-667.	3.2	113
141	Facile Synthesis of Mesoporous TiO2â^'C Nanosphere as an Improved Anode Material for Superior High Rate 1.5 V Rechargeable Li Ion Batteries Containing LiFePO4â^'C Cathode. Journal of Physical Chemistry C, 2010, 114, 10308-10313.	1.5	113
142	Interfacial design for lithium–sulfur batteries: From liquid to solid. EnergyChem, 2019, 1, 100002.	10.1	113
143	In SituScanning Tunneling Microscopy of Benzene, Naphthalene, and Anthracene Adsorbed on Cu(111) in Solution. Langmuir, 1997, 13, 7173-7179.	1.6	111
144	Specific Aptamerâ^'Protein Interaction Studied by Atomic Force Microscopy. Analytical Chemistry, 2003, 75, 2112-2116.	3.2	111

#	Article	IF	CITATIONS
145	High Performance Photodetectors of Individual InSe Single Crystalline Nanowire. Journal of the American Chemical Society, 2009, 131, 15602-15603.	6.6	108
146	Wet Chemistry Synthesis of Multidimensional Nanocarbon–Sulfur Hybrid Materials with Ultrahigh Sulfur Loading for Lithium–Sulfur Batteries. ACS Applied Materials & Interfaces, 2016, 8, 3584-3590.	4.0	108
147	Hydrothermal reduction of three-dimensional graphene oxide for binder-free flexible supercapacitors. Journal of Materials Chemistry A, 2014, 2, 10830.	5.2	107
148	Progress in the sustainable recycling of spent lithiumâ€ion batteries. SusMat, 2021, 1, 241-254.	7.8	104
149	Configurations of a Calix[8]arene and a C60/Calix[8]arene Complex on a Au(111) Surface. Angewandte Chemie - International Edition, 2003, 42, 2747-2751.	7.2	103
150	TiO2-Based Composite Nanotube Arrays Prepared via Layer-by-Layer Assembly. Advanced Functional Materials, 2005, 15, 196-202.	7.8	103
151	Tuning the Fermi-level of TiO ₂ mesoporous layer by lanthanum doping towards efficient perovskite solar cells. Nanoscale, 2016, 8, 16881-16885.	2.8	103
152	Carbonizedâ€MOF as a Sulfur Host for Aluminum–Sulfur Batteries with Enhanced Capacity and Cycling Life. Advanced Functional Materials, 2019, 29, 1807676.	7.8	103
153	Facile Synthesis of Germanium Nanocrystals and Their Application in Organic–Inorganic Hybrid Photodetectors. Advanced Materials, 2011, 23, 3704-3707.	11.1	102
154	Structural engineering of SnS2/Graphene nanocomposite for high-performance K-ion battery anode. Nano Energy, 2019, 60, 912-918.	8.2	101
155	Single Nanowire Electrode Electrochemistry of Silicon Anode by in Situ Atomic Force Microscopy: Solid Electrolyte Interphase Growth and Mechanical Properties. ACS Applied Materials & Interfaces, 2014, 6, 20317-20323.	4.0	100
156	Potential-Induced Phase Transition of Trimesic Acid Adlayer on Au(111). Journal of Physical Chemistry B, 2004, 108, 1931-1937.	1.2	99
157	In Situ Electrochemical Regeneration of Degraded LiFePO ₄ Electrode with Functionalized Prelithiation Separator. Advanced Energy Materials, 2022, 12, .	10.2	99
158	Controllable Preparation of Submicrometer Single-Crystal C60Rods and Tubes Trough Concentration Depletion at the Surfaces of Seeds. Journal of Physical Chemistry C, 2007, 111, 10498-10502.	1.5	98
159	Physical vapor deposition of amorphous MoS ₂ nanosheet arrays on carbon cloth for highly reproducible large-area electrocatalysts for the hydrogen evolution reaction. Journal of Materials Chemistry A, 2015, 3, 19277-19281.	5.2	97
160	Bandgap Engineering of Monodispersed Cu _{2–<i>x</i>} S _{<i>y</i>} Se _{1–<i>y</i>} Nanocrystals through Chalcogen Ratio and Crystal Structure. Journal of the American Chemical Society, 2011, 133, 18558-18561.	6.6	96
161	Increased residual lithium compounds guided design for green recycling of spent lithium-ion cathodes. Energy and Environmental Science, 2021, 14, 1461-1468.	15.6	96
162	Simulation of Water Cluster Assembly on a Graphite Surface. Journal of Physical Chemistry B, 2005, 109, 14183-14188.	1.2	95

#	Article	IF	CITATIONS
163	Oneâ€Nanometerâ€Precision Control of Al ₂ O ₃ Nanoshells through a Solutionâ€Based Synthesis Route. Angewandte Chemie - International Edition, 2014, 53, 12776-12780.	7.2	95
164	Confining Iron Carbide Nanocrystals inside CN _{<i>x</i>} @CNT toward an Efficient Electrocatalyst for Oxygen Reduction Reaction. ACS Applied Materials & Interfaces, 2015, 7, 11508-11515.	4.0	94
165	A Flexible Solid Electrolyte with Multilayer Structure for Sodium Metal Batteries. Advanced Energy Materials, 2020, 10, 1903966.	10.2	94
166	Tin/Platinum Bimetallic Nanotube Array and its Electrocatalytic Activity for Methanol Oxidation. Advanced Materials, 2005, 17, 746-750.	11.1	93
167	Nitrogen, phosphorus and sulfur co-doped ultrathin carbon nanosheets as a metal-free catalyst for selective oxidation of aromatic alkanes and the oxygen reduction reaction. Journal of Materials Chemistry A, 2016, 4, 18470-18477.	5.2	93
168	In Situ Scanning Tunneling Microscopy of Well-Defined Ir(111) Surface:Â High-Resolution Imaging of Adsorbed Sulfate. Journal of Physical Chemistry B, 1999, 103, 6978-6983.	1.2	92
169	In situ STM imaging of surface dissolution and rearrangement of a Pt–Fe alloy electrocatalyst in electrolyte solution. Chemical Communications, 2002, , 58-59.	2.2	92
170	Ruthenium/Graphene-like Layered Carbon Composite as an Efficient Hydrogen Evolution Reaction Electrocatalyst. ACS Applied Materials & amp; Interfaces, 2016, 8, 35132-35137.	4.0	92
171	Chiral Hierarchical Molecular Nanostructures on Two-Dimensional Surface by Controllable Trinary Self-Assembly. Journal of the American Chemical Society, 2011, 133, 21010-21015.	6.6	91
172	C64H4:Â Production, Isolation, and Structural Characterizations of a Stable Unconventional Fulleride. Journal of the American Chemical Society, 2006, 128, 6605-6610.	6.6	90
173	Encapsulation of Sulfur in a Hollow Porous Carbon Substrate for Superior Liâ€5 Batteries with Long Lifespan. Particle and Particle Systems Characterization, 2013, 30, 321-325.	1.2	90
174	Sodium chloride-assisted green synthesis of a 3D Fe–N–C hybrid as a highly active electrocatalyst for the oxygen reduction reaction. Journal of Materials Chemistry A, 2016, 4, 7781-7787.	5.2	88
175	Mesoscopic self-organization of a self-assembled supramolecular rectangle on highly oriented pyrolytic graphite and Au(111) surfaces. Proceedings of the National Academy of Sciences of the United States of America, 2005, 102, 971-974.	3.3	86
176	Boosting the Open Circuit Voltage and Fill Factor of QDSSCs Using Hierarchically Assembled ITO@Cu ₂ S Nanowire Array Counter Electrodes. Nano Letters, 2015, 15, 3088-3095.	4.5	86
177	Designing solid-state interfaces on lithium-metal anodes: a review. Science China Chemistry, 2019, 62, 1286-1299.	4.2	86
178	2D Assembly of Metallacycles on HOPG by Shape-Persistent Macrocycle Templates. Journal of the American Chemical Society, 2010, 132, 1328-1333.	6.6	85
179	Dimerization of Sulfur Headgroups in 4-Mercaptopyridine Self-Assembled Monolayers on Au(111) Studied by Scanning Tunneling Microscopy. Journal of Physical Chemistry B, 1998, 102, 5943-5946.	1.2	84
180	Suppressing the P2–O2 Phase Transition of Na _{0.67} Mn _{0.67} Ni _{0.33} O ₂ by Magnesium Substitution for Improved Sodiumâ€ion Batteries. Angewandte Chemie, 2016, 128, 7571-7575.	1.6	84

#	Article	IF	CITATIONS
181	A Black Phosphorus–Graphite Composite Anode for Liâ€/Naâ€/Kâ€Ion Batteries. Angewandte Chemie - International Edition, 2020, 59, 2318-2322.	7.2	84
182	Enabling a Durable Electrochemical Interface via an Artificial Amorphous Cathode Electrolyte Interphase for Hybrid Solid/Liquid Lithiumâ€Metal Batteries. Angewandte Chemie - International Edition, 2020, 59, 6585-6589.	7.2	84
183	Control of Supramolecular Rectangle Self-Assembly with a Molecular Template. Journal of the American Chemical Society, 2007, 129, 9268-9269.	6.6	83
184	Phase Control on Surface for the Stabilization of High Energy Cathode Materials of Lithium Ion Batteries. Journal of the American Chemical Society, 2019, 141, 4900-4907.	6.6	83
185	Self-Organization of a Self-Assembled Supramolecular Rectangle, Square, and Three-Dimensional Cage on Au(111) Surfaces. Journal of the American Chemical Society, 2005, 127, 16279-16286.	6.6	82
186	Controllable crystalline structure of fullerenenanorods and transport properties of an individual nanorod. Journal of Materials Chemistry, 2008, 18, 328-332.	6.7	82
187	Urchin-like Au@CdS/WO ₃ micro/nano heterostructure as a visible-light driven photocatalyst for efficient hydrogen generation. Chemical Communications, 2015, 51, 13842-13845.	2.2	82
188	A Flexible Solid Electrolyte Interphase Layer for Long‣ife Lithium Metal Anodes. Angewandte Chemie, 2018, 130, 1521-1525.	1.6	82
189	Niâ^'Pt Multilayered Nanowire Arrays with Enhanced Coercivity and High Remanence Ratio. Inorganic Chemistry, 2005, 44, 3013-3015.	1.9	81
190	Click and Patterned Functionalization of Graphene by Diels–Alder Reaction. Journal of the American Chemical Society, 2016, 138, 7448-7451.	6.6	81
191	Investigation of Physical and Electronic Properties of GeSe for Photovoltaic Applications. Advanced Electronic Materials, 2017, 3, 1700141.	2.6	81
192	Atom-Thick Interlayer Made of CVD-Grown Graphene Film on Separator for Advanced Lithium–Sulfur Batteries. ACS Applied Materials & Interfaces, 2017, 9, 43696-43703.	4.0	79
193	Single-Molecule Imaging of Iron-Phthalocyanine-Catalyzed Oxygen Reduction Reaction by <i>in Situ</i> Scanning Tunneling Microscopy. ACS Nano, 2016, 10, 8746-8750.	7.3	78
194	New Structure ofl-Cysteine Self-Assembled Monolayer on Au(111):Â Studies by In Situ Scanning Tunneling Microscopy. Langmuir, 2001, 17, 6203-6206.	1.6	77
195	Silicon-based nanomaterials for lithium-ion batteries. Science Bulletin, 2012, 57, 4104-4110.	1.7	77
196	AFM and STM study of \hat{I}^2 -amyloid aggregation on graphite. Ultramicroscopy, 2003, 97, 73-79.	0.8	76
197	Facile growth of centimeter-sized single-crystal graphene on copper foil at atmospheric pressure. Journal of Materials Chemistry C, 2015, 3, 3530-3535.	2.7	76
198	Rechargeable dual-metal-ion batteries for advanced energy storage. Physical Chemistry Chemical Physics, 2016, 18, 9326-9333.	1.3	76

#	Article	IF	CITATIONS
199	Confined Synthesis of acis-Isotactic Ladder Polysilsesquioxane by Using a π-Stacking and H-Bonding Superstructure. Angewandte Chemie - International Edition, 2006, 45, 3112-3116.	7.2	74
200	High-Thermal- and Air-Stability Cathode Material with Concentration-Gradient Buffer for Li-Ion Batteries. ACS Applied Materials & Interfaces, 2017, 9, 42829-42835.	4.0	74
201	In situ nitrogen-doped nanoporous carbon nanocables as an efficient metal-free catalyst for oxygen reduction reaction. Journal of Materials Chemistry A, 2014, 2, 10154.	5.2	73
202	Three-dimensional nanostructured electrodes for efficient quantum-dot-sensitized solar cells. Nano Energy, 2017, 32, 130-156.	8.2	73
203	Selective Extraction of Transition Metals from Spent LiNi _{<i>x</i>} Co _y Mn _{1â~<i>x</i>â~<i>y</i>} O ₂ Cathode via Regulation of Coordination Environment. Angewandte Chemie - International Edition, 2022, 61, .	7.2	72
204	Ordered Adlayers of Organic Molecules on Sulfur-Modified Au(111):Â In Situ Scanning Tunneling Microscopy Study. Langmuir, 2000, 16, 2164-2168.	1.6	70
205	Wet chemical synthesis of Cu/TiO2 nanocomposites with integrated nano-current-collectors as high-rate anode materials in lithium-ion batteries. Physical Chemistry Chemical Physics, 2011, 13, 2014.	1.3	70
206	Microbial-Phosphorus-Enabled Synthesis of Phosphide Nanocomposites for Efficient Electrocatalysts. Journal of the American Chemical Society, 2017, 139, 11248-11253.	6.6	70
207	Micromechanism in All-Solid-State Alloy-Metal Batteries: Regulating Homogeneous Lithium Precipitation and Flexible Solid Electrolyte Interphase Evolution. Journal of the American Chemical Society, 2021, 143, 839-848.	6.6	70
208	Ultra-thin solid electrolyte interphase evolution and wrinkling processes in molybdenum disulfide-based lithium-ion batteries. Nature Communications, 2019, 10, 3265.	5.8	69
209	Electrochemical Scanning Tunneling Microscopy:  Adlayer Structure and Reaction at Solid/liquid Interface. Journal of Physical Chemistry C, 2007, 111, 16109-16130.	1.5	68
210	Cooperative Shielding of Bi-Electrodes via In Situ Amorphous Electrode–Electrolyte Interphases for Practical High-Energy Lithium-Metal Batteries. Journal of the American Chemical Society, 2021, 143, 16768-16776.	6.6	68
211	Phaseâ€Controlled Synthesis of 1Tâ€MoSe ₂ /NiSe Heterostructure Nanowire Arrays via Electronic Injection for Synergistically Enhanced Hydrogen Evolution. Small Methods, 2019, 3, 1800317.	4.6	67
212	Well-Defined Fullerene Nanowire Arrays. Advanced Functional Materials, 2003, 13, 626-630.	7.8	66
213	Functionalized carbon nanotubes as sensitive materials for electrochemical detection of ultra-trace 2,4,6-trinitrotoluene. Physical Chemistry Chemical Physics, 2006, 8, 3567.	1.3	66
214	In Situ Observation of Electrolyte-Concentration-Dependent Solid Electrolyte Interphase on Graphite in Dimethyl Sulfoxide. ACS Applied Materials & Interfaces, 2015, 7, 9573-9580.	4.0	66
215	Synergistic Electrocatalysts for Alkaline Hydrogen Oxidation and Evolution Reactions. Advanced Functional Materials, 2022, 32, 2107479.	7.8	66
216	A Novel β-CDâ^'Hemin Complex Photocatalyst for Efficient Degradation of Organic Pollutants at Neutral pHs under Visible Irradiation. Journal of Physical Chemistry B, 2003, 107, 9409-9414.	1.2	65

#	Article	IF	CITATIONS
217	Non-sacrificial template synthesis of Cr2O3–C hierarchical core/shell nanospheres and their application as anode materials in lithium-ion batteries. Journal of Materials Chemistry, 2010, 20, 7565.	6.7	65
218	Controlling the Reaction of Nanoparticles for Hollow Metal Oxide Nanostructures. Journal of the American Chemical Society, 2018, 140, 9070-9073.	6.6	65
219	An Ordered Ni ₆ â€Ring Superstructure Enables a Highly Stable Sodium Oxide Cathode. Advanced Materials, 2019, 31, e1903483.	11.1	65
220	Gold/Titania Core/Sheath Nanowires Prepared by Layer-by-Layer Assembly. Journal of Physical Chemistry B, 2003, 107, 5441-5444.	1.2	64
221	Controllable Distribution of Single Molecules and Peptides within Oligomer Template Investigated by STM. Journal of the American Chemical Society, 2006, 128, 12384-12385.	6.6	64
222	A rechargeable aqueous aluminum–sulfur battery through acid activation in water-in-salt electrolyte. Chemical Communications, 2020, 56, 2023-2026.	2.2	64
223	STM investigation of the dependence of alkane and alkane (C18H38, C19H40) derivatives self-assembly on molecular chemical structure on HOPG surface. Surface Science, 2008, 602, 1256-1266.	0.8	63
224	Designed synthesis of SnO2–C hollow microspheres as an anode material for lithium-ion batteries. Chemical Communications, 2017, 53, 11189-11192.	2.2	63
225	Stabilizing Cathode Materials of Lithium-Ion Batteries by Controlling Interstitial Sites on the Surface. CheM, 2018, 4, 1685-1695.	5.8	63
226	Kinetic Origin of Planar Gliding in Single-Crystalline Ni-Rich Cathodes . Journal of the American Chemical Society, 2022, 144, 11338-11347.	6.6	63
227	Interface Assembly Synthesis of Inorganic Composite Hollow Spheres. Journal of Physical Chemistry B, 2004, 108, 9734-9738.	1.2	62
228	Isomeric Routes to Schiffâ€Base Singleâ€layered Covalent Organic Frameworks. Small, 2014, 10, 4934-4939.	5.2	62
229	Highly Dispersed Metal Nanoparticles in Porous Anodic Alumina Films Prepared by a Breathing Process of Polyacrylamide Hydrogel. Chemistry of Materials, 2003, 15, 4332-4336.	3.2	61
230	Molecular Evidence for the Catalytic Process of Cobalt Porphyrin Catalyzed Oxygen Evolution Reaction in Alkaline Solution. Journal of the American Chemical Society, 2019, 141, 7665-7669.	6.6	61
231	Optimizing the carbon coating on LiFePO4 for improved battery performance. RSC Advances, 2014, 4, 7795.	1.7	60
232	Accurate surface control of core–shell structured LiMn _{0.5} Fe _{0.5} PO ₄ @C for improved battery performance. Journal of Materials Chemistry A, 2014, 2, 17359-17365.	5.2	60
233	Revealing the Surface Effect of the Soluble Catalyst on Oxygen Reduction/Evolution in Li–O ₂ Batteries. Journal of the American Chemical Society, 2019, 141, 6900-6905.	6.6	60
234	A Covalent Organic Framework Film for Threeâ€State Nearâ€Infrared Electrochromism and a Molecular Logic Gate. Angewandte Chemie - International Edition, 2021, 60, 12498-12503.	7.2	60

#	Article	IF	CITATIONS
235	Dynamics of adsorption and phase formation of p-nitrobenzoic acid at Au(111) surface in solution: A combined surface-enhanced infrared and STM study. Physical Chemistry Chemical Physics, 2001, 3, 3336-3342.	1.3	59
236	From a Lamellar to Hexagonal Self-Assembly of Bis(4,4′-(m,m′-di(dodecyloxy)phenyl)-2,2′-difluoro-1,3,2-dioxaborin) Molecules: Atrans-to-cis-Isomerization-Induced Structural Transition Studied with STM. Angewandte Chemie - International Edition, 2006, 45, 3996-4000.	7.2	59
237	Stabilizing Polymer–Lithium Interface in a Rechargeable Solid Battery. Advanced Functional Materials, 2020, 30, 1908047.	7.8	59
238	Interfacial Evolution of Lithium Dendrites and Their Solid Electrolyte Interphase Shells of Quasiâ€Solidâ€State Lithiumâ€Metal Batteries. Angewandte Chemie - International Edition, 2020, 59, 18120-18125.	7.2	59
239	Promoting crystalline grain growth and healing pinholes by water vapor modulated post-annealing for enhancing the efficiency of planar perovskite solar cells. Journal of Materials Chemistry A, 2016, 4, 13458-13467.	5.2	58
240	Dynamic Evolution of a Cathode Interphase Layer at the Surface of LiNi _{0.5} Co _{0.2} Mn _{0.3} O ₂ in Quasi-Solid-State Lithium Batteries. Journal of the American Chemical Society, 2020, 142, 20752-20762.	6.6	58
241	Morphology and modulus evolution of graphite anode in lithium ion battery: An in situ AFM investigation. Science China Chemistry, 2014, 57, 178-183.	4.2	57
242	Constructing Stable Chromenoquinoline-Based Covalent Organic Frameworks via Intramolecular Povarov Reaction. Journal of the American Chemical Society, 2022, 144, 2488-2494.	6.6	57
243	Scanning tunneling microscopy of the formation, transformation, and property of oligothiophene self-organizations on graphite and gold surfaces. Proceedings of the National Academy of Sciences of the United States of America, 2007, 104, 3707-3712.	3.3	56
244	Helical Molecular Duplex Strands:Â Multiple Hydrogen-Bond-Mediated Assembly of Self-Complementary Oligomeric Hydrazide Derivatives. Journal of Organic Chemistry, 2007, 72, 4936-4946.	1.7	56
245	Controllable Synthesis of Hollow Hierarchical Palladium Nanostructures with Enhanced Activity for Proton/Hydrogen Sensing. Journal of Physical Chemistry C, 2008, 112, 338-344.	1.5	56
246	Solvent-Controlled 2D Hostâ^'Guest (2,7,12-Trihexyloxytruxene/Coronene) Molecular Nanostructures at Organic Liquid/Solid Interface Investigated by Scanning Tunneling Microscopy. Langmuir, 2010, 26, 8195-8200.	1.6	56
247	Solvent-Induced Oriented Attachment Growth of Air-Stable Phase-Pure Pyrite FeS ₂ Nanocrystals. Journal of the American Chemical Society, 2015, 137, 2211-2214.	6.6	56
248	Improving the structural stability of Li-rich cathode materials via reservation of cations in the Li-slab for Li-ion batteries. Nano Research, 2017, 10, 4201-4209.	5.8	56
249	Advanced transition metal/nitrogen/carbon-based electrocatalysts for fuel cell applications. Science China Chemistry, 2020, 63, 1517-1542.	4.2	56
250	Inâ€Situ Scanning Tunneling Microscopy of Cobaltâ€Phthalocyanineâ€Catalyzed CO ₂ Reduction Reaction. Angewandte Chemie - International Edition, 2020, 59, 16098-16103.	7.2	56
251	A novel air-stable n-type organic semiconductor: 4,4′-bis[(6,6′-diphenyl)-2,2-difluoro-1,3,2-dioxaborine] and its application in organic ambipolar field-effect transistors. Journal of Materials Chemistry, 2006, 16, 4499-4503.	6.7	55
252	Engineering of Linear Molecular Nanostructures by a Hydrogen-Bond-Mediated Modular and Flexible Hostâ''Guest Assembly. ACS Nano, 2010, 4, 5685-5692.	7.3	55

#	Article	IF	CITATIONS
253	Tuning the branches and composition of PtCu nanodendrites through underpotential deposition of Cu towards advanced electrocatalytic activity. Journal of Materials Chemistry A, 2017, 5, 9014-9021.	5.2	55
254	Synthesis and characterization of 3D double branched K junction carbon nanotubes and nanorods. Carbon, 2007, 45, 268-273.	5.4	53
255	Molecular Conductance through a Quadrupleâ€Hydrogenâ€Bondâ€Bridged Supramolecular Junction. Angewandte Chemie - International Edition, 2016, 55, 12393-12397.	7.2	53
256	Heterogeneous nucleation and growth of highly crystalline imine-linked covalent organic frameworks. Chemical Communications, 2018, 54, 5976-5979.	2.2	53
257	Improving the stability of LiNi0.80Co0.15Al0.05O2 by AlPO4 nanocoating for lithium-ion batteries. Science China Chemistry, 2017, 60, 1230-1235.	4.2	52
258	In situ scanning tunneling microscopy of Cu(110): atomic structures of halide adlayers and anodic dissolution. Journal of Electroanalytical Chemistry, 1999, 473, 10-18.	1.9	51
259	Time-resolved surface-enhanced infra-red study of molecular adsorption at the electrochemical interface. Surface Science, 1999, 427-428, 190-194.	0.8	51
260	Self-assembled two-dimensional hexagonal networks. Journal of Materials Chemistry, 2002, 12, 2856-2858.	6.7	51
261	Self-Assembling of an Amphiphilic Polyacetylene Carryingl-Leucine Pendants:Â A Homopolymer Case. Macromolecules, 2003, 36, 5447-5450.	2.2	51
262	Effect of cations in ionic liquids on the electrochemical performance of lithium-sulfur batteries. Science China Chemistry, 2014, 57, 1564-1569.	4.2	51
263	Two-dimensional chiral molecular assembly on solid surfaces: formation and regulation. National Science Review, 2015, 2, 205-216.	4.6	51
264	In-situ scanning tunneling microscopy of well-ordered Rh(111) electrodes. Journal of Electroanalytical Chemistry, 1995, 381, 105-111.	1.9	50
265	Study of Citrate Adsorbed on the Au(111) Surface by Scanning Probe Microscopy. Langmuir, 2003, 19, 10000-10003.	1.6	50
266	Self-Assembly of PcOC8 and Its Sandwich Lanthanide Complex Pr(PcOC8)2with Oligo(Phenylene-ethynylene) Molecules. Journal of Physical Chemistry B, 2005, 109, 19859-19865.	1.2	50
267	One Solvent Induces a Series of Structural Transitions in Monodendron Molecular Selfâ€Assembly from Lamellar to Quadrangular to Hexagonal. Chemistry - A European Journal, 2009, 15, 9669-9673.	1.7	50
268	Chiral Kagome Network from Thiacalix[4]arene Tetrasulfonate at the Interface of Aqueous Solution/Au(111) Surface: An in Situ Electrochemical Scanning Tunneling Microscopy Study. Journal of the American Chemical Society, 2010, 132, 5598-5599.	6.6	50
269	From biological enzyme to single atomic Fe–N–C electrocatalyst for efficient oxygen reduction. Chemical Communications, 2018, 54, 1307-1310.	2.2	50
270	Facile solution synthesis of hexagonal Alq3 nanorods and their field emission properties. Chemical Communications, 2007, , 3083.	2.2	49

#	Article	IF	CITATIONS
271	Morphology control and shape evolution in 3D hierarchical superstructures. Science China Chemistry, 2012, 55, 2249-2256.	4.2	49
272	Tunable structure and dynamics of solid electrolyte interphase at lithium metal anode. Nano Energy, 2020, 75, 104967.	8.2	48
273	Recent Advances on Nonprecious-Metal-Based Bifunctional Oxygen Electrocatalysts for Zinc–Air Batteries. Energy & Fuels, 2021, 35, 6380-6401.	2.5	48
274	Self-deposition of Pt nanocrystals on Mn3O4 coated carbon nanotubes for enhanced oxygen reduction electrocatalysis. Journal of Materials Chemistry A, 2013, 1, 7463.	5.2	47
275	Bilayer Molecular Assembly at a Solid/Liquid Interface as Triggered by a Mild Electric Field. Angewandte Chemie - International Edition, 2014, 53, 13395-13399.	7.2	47
276	Metal–Organic Polyhedra Cages Immobilized on a Plasmonic Substrate for Sensitive Detection of Trace Explosives. Advanced Functional Materials, 2015, 25, 6009-6017.	7.8	47
277	Progress of electrode/electrolyte interfacial investigation of Li-ion batteries via in situ scanning probe microscopy. Science Bulletin, 2015, 60, 839-849.	4.3	47
278	Synergy of Black Phosphorus–Graphite–Polyaniline-Based Ternary Composites for Stable High Reversible Capacity Na-Ion Battery Anodes. ACS Applied Materials & Interfaces, 2019, 11, 16656-16661.	4.0	46
279	Confinement Strategies for Precise Synthesis of Efficient Electrocatalysts from the Macroscopic to the Atomic Level. Accounts of Materials Research, 2021, 2, 907-919.	5.9	46
280	Electrocatalytic Hydrogen Oxidation in Alkaline Media: From Mechanistic Insights to Catalyst Design. ACS Nano, 2022, 16, 5153-5183.	7.3	46
281	Structural selection of graphene supramolecular assembly oriented by molecular conformation and alkyl chain. Proceedings of the National Academy of Sciences of the United States of America, 2008, 105, 16849-16854.	3.3	45
282	Nitroxide radical polymer/graphene nanocomposite as an improved cathode material for rechargeable lithium batteries. Electrochimica Acta, 2012, 72, 81-86.	2.6	45
283	Highâ€Temperature Formation of a Functional Film at the Cathode/Electrolyte Interface in Lithium–Sulfur Batteries: An Inâ€Situ AFM Study. Angewandte Chemie - International Edition, 2017, 56, 14433-14437.	7.2	45
284	Solvent Effects on the Chirality in Two-Dimensional Molecular Assemblies. Journal of Physical Chemistry B, 2003, 107, 747-750.	1.2	44
285	STM Study of Two-Dimensional Assemblies of Tricarboxylic Acid Derivatives on Au(111). Journal of Physical Chemistry B, 2004, 108, 11251-11255.	1.2	43
286	Structural Diversity of a Monodendron Molecule Self-Assembly in Different Solvents Investigated by Scanning Tunneling Microscopy: From Dispersant to Counterpart. Journal of Physical Chemistry C, 2009, 113, 16193-16198.	1.5	43
287	Self-assembly and aggregation of melamine and melamine–uric/cyanuric acid investigated by STM and AFM on solid surfaces. Physical Chemistry Chemical Physics, 2009, 11, 7708.	1.3	43
288	Hanging Pt hollow nanocrystal assemblies on graphene resulting in an enhanced electrocatalyst. Chemical Communications, 2012, 48, 10331.	2.2	43

#	Article	IF	CITATIONS
289	General Synthetic Strategy for Hollow Hybrid Microspheres through a Progressive Inward Crystallization Process. Journal of the American Chemical Society, 2016, 138, 5916-5922.	6.6	43
290	Precise Surface Engineering of Cathode Materials for Improved Stability of Lithiumâ€kon Batteries. Small, 2019, 15, e1901019.	5.2	43
291	Rechargeable Aluminium–Sulfur Battery with Improved Electrochemical Performance by Cobaltâ€Containing Electrocatalyst. Angewandte Chemie - International Edition, 2020, 59, 22963-22967.	7.2	43
292	Eco-friendly visible-wavelength photodetectors based on bandgap engineerable nanomaterials. Journal of Materials Chemistry, 2011, 21, 17582.	6.7	42
293	Integrated Prototype Nanodevices via SnO2 Nanoparticles Decorated SnSe Nanosheets. Scientific Reports, 2013, 3, 2613.	1.6	42
294	In vitro and in vivo photothermally enhanced chemotherapy by single-walled carbon nanohorns as a drug delivery system. Journal of Materials Chemistry B, 2014, 2, 4726-4732.	2.9	41
295	Surface Zn doped LiMn ₂ O ₄ for an improved high temperature performance. Chemical Communications, 2018, 54, 5326-5329.	2.2	41
296	Advancing to 4.6ÂV Review and Prospect in Developing Highâ€Energyâ€Density LiCoO ₂ Cathode for Lithiumâ€Ion Batteries. Small Methods, 2022, 6, e2200148.	4.6	41
297	Adsorption and ordered phase formation of 2,2′-bypyridine on Au(111): a combined surface-enhanced infrared and STM study. Journal of Electroanalytical Chemistry, 2000, 481, 62-68.	1.9	40
298	ZnOEP based phototransistor: signal amplification and light-controlled switch. Chemical Communications, 2008, , 2653.	2.2	40
299	Direct Visualization of Nucleation and Growth Processes of Solid Electrolyte Interphase Film Using in Situ Atomic Force Microscopy. ACS Applied Materials & amp; Interfaces, 2017, 9, 22063-22067.	4.0	40
300	Direct insights into the electrochemical processes at anode/electrolyte interfaces in magnesium-sulfur batteries. Nano Energy, 2018, 49, 453-459.	8.2	40
301	Surface Mechanism of Catalytic Electrodes in Lithium-Oxygen Batteries: How Nanostructures Mediate the Interfacial Reactions. Journal of the American Chemical Society, 2020, 142, 16007-16015.	6.6	40
302	Insights into electrocatalysis by scanning tunnelling microscopy. Chemical Society Reviews, 2021, 50, 5832-5849.	18.7	40
303	Controlled Orientation of Individual Molecules by Electrode Potentials. ChemPhysChem, 2001, 2, 617-619.	1.0	39
304	Time-Dependent Organization and Wettability of Decanethiol Self-Assembled Monolayer on Au(111) Investigated with STM. Journal of Physical Chemistry B, 2006, 110, 1794-1799.	1.2	39
305	Aqueous route for mesoporous metal oxides using inorganic metal source and their applications. Microporous and Mesoporous Materials, 2007, 100, 233-240.	2.2	39
306	Structure and structural transition of chiral domains in oligo(p-phenylenevinylene) assembly investigated by scanning tunneling microscopy. Proceedings of the National Academy of Sciences of the United States of America, 2010, 107, 2769-2774.	3.3	39

#	Article	IF	CITATIONS
307	Core–shell structured Ce ₂ S ₃ @ZnO and its potential as a pigment. Journal of Materials Chemistry A, 2015, 3, 2176-2180.	5.2	39
308	Influence of <i>N</i> , <i>N</i> -Dimethylformamide Annealing on the Local Electrical Properties of Organometal Halide Perovskite Solar Cells: an Atomic Force Microscopy Investigation. ACS Applied Materials & Interfaces, 2016, 8, 26002-26007.	4.0	39
309	Manipulating Particle Chemistry for Hollow Carbon-based Nanospheres: Synthesis Strategies, Mechanistic Insights, and Electrochemical Applications. Accounts of Chemical Research, 2021, 54, 221-231.	7.6	39
310	Light-Induced Structural Transformation in Self-Assembled Monolayer of 4-(Amyloxy)cinnamic Acid Investigated with Scanning Tunneling Microscopy. Journal of Physical Chemistry B, 2005, 109, 14773-14778.	1.2	38
311	Scanning Tunneling Microscopy Investigation of a Supramolecular Self-Assembled Three-Dimensional Chiral Prism on a Au(111) Surface. Journal of the American Chemical Society, 2008, 130, 8878-8879.	6.6	38
312	Nanopatterning of Donor/Acceptor Hybrid Supramolecular Architectures on Highly Oriented Pyrolytic Graphite: A Scanning Tunneling Microscopy Study. Journal of the American Chemical Society, 2008, 130, 13433-13441.	6.6	38
313	A facile method for preparing one-molecule-thick free-standing organic nanosheets with a regular square shape. Chemical Communications, 2010, 46, 725-727.	2.2	38
314	Polyethylene glycol-directed SnO2 nanowires for enhanced gas-sensing properties. Nanoscale, 2011, 3, 1802.	2.8	38
315	Ladderlike carbon nanoarrays on 3D conducting skeletons enable uniform lithium nucleation for stable lithium metal anodes. Chemical Communications, 2018, 54, 5330-5333.	2.2	38
316	Progress in the Mechanisms and Materials for CO ₂ Electroreduction toward C ₂₊ Products. Wuli Huaxue Xuebao/ Acta Physico - Chimica Sinica, 2020, 36, 1906085-0.	2.2	38
317	Coordination-Assisted Precise Construction of Metal Oxide Nanofilms for High-Performance Solid-State Batteries. Journal of the American Chemical Society, 2022, 144, 2179-2188.	6.6	38
318	Effect of solution pH on the structure of a 4-mercaptopyridine monolayer self-assembled on Au(111). Journal of Electroanalytical Chemistry, 2000, 489, 68-75.	1.9	37
319	Modular Assembly of Alkyl-Substituted Phthalocyanines with 1-lodooctadecane. Chemistry of Materials, 2002, 14, 2837-2838.	3.2	37
320	Molecular Trapping Phenomenon of the 2-D Assemblies of Octa-Alkoxyl-Substituted Phthalocyanine Studied by Scanning Tunneling Microscopy. Journal of Physical Chemistry B, 2002, 106, 12569-12574.	1.2	37
321	Adsorbed Structures of 4,4â€~-Bipyridine on Cu(111) in Acid Studied by STM and IR. Langmuir, 2006, 22, 3640-3646.	1.6	37
322	Zero discharge process for foil industry waste acid reclamation: Coupling of diffusion dialysis and electrodialysis with bipolar membranes. Journal of Membrane Science, 2013, 432, 90-96.	4.1	37
323	Controlled Formation of Metal@Al ₂ O ₃ Yolk–Shell Nanostructures with Improved Thermal Stability. ACS Applied Materials & Interfaces, 2015, 7, 27031-27034.	4.0	37
324	Single-Molecule Conductance through an Isoelectronic B–N Substituted Phenanthrene Junction. Journal of the American Chemical Society, 2020, 142, 8068-8073.	6.6	37

#	Article	IF	CITATIONS
325	Synthesis of Covalent Organic Framework Films at Interfaces. Bulletin of the Chemical Society of Japan, 2021, 94, 1090-1098.	2.0	37
326	Morphology control of Fe ₂ O ₃ nanocrystals and their application in catalysis. Nanotechnology, 2007, 18, 385605.	1.3	36
327	Ionâ€Transferâ€Based Growth: A Mechanism for CuTCNQ Nanowire Formation. Advanced Materials, 2008, 20, 4879-4882.	11.1	36
328	pH-Responsive Mechanism of a Deoxycholic Acid and Folate Comodified Chitosan Micelle under Cancerous Environment. Journal of Physical Chemistry B, 2013, 117, 1261-1268.	1.2	36
329	In situ encapsulation of Pd inside the MCM-41 channel. Chemical Communications, 2015, 51, 7482-7485.	2.2	36
330	Substrate Orientation Effect in the On-Surface Synthesis of Tetrathiafulvalene-Integrated Single-Layer Covalent Organic Frameworks. Langmuir, 2015, 31, 11755-11759.	1.6	36
331	Nano/Micro‣tructured Si/C Anodes with High Initial Coulombic Efficiency in Li″on Batteries. Chemistry - an Asian Journal, 2016, 11, 1205-1209.	1.7	36
332	Interfacial Strain Engineering in Wide-Bandgap GeS Thin Films for Photovoltaics. Journal of the American Chemical Society, 2021, 143, 9664-9671.	6.6	36
333	Template Synthesis of Sc@C82(I) Nanowires and Nanotubes at Room Temperature. Advanced Materials, 2005, 17, 71-73.	11.1	35
334	Câ^'H··Â-F Hydrogen Bonding: The Origin of the Self-Assemblies of Bis(2,2'-difluoro-1,3,2-dioxaborine). Langmuir, 2006, 22, 4750-4757.	1.6	35
335	TiN nanocrystal anchored on N-doped graphene as effective sulfur hosts for high-performance lithium-sulfur batteries. Journal of Energy Chemistry, 2021, 54, 16-22.	7.1	35
336	The two-dimensional self-assembled n-alkoxy-substituted stilbenoid compounds and triphenylenes studied by scanning tunneling microscopy. Surface Science, 2003, 538, L451-L459.	0.8	34
337	Initial solid electrolyte interphase formation process of graphite anode in LiPF6 electrolyte: an in situ ECSTM investigation. Physical Chemistry Chemical Physics, 2012, 14, 7330.	1.3	34
338	Crystallinityâ€Modulated Electrocatalytic Activity of a Nickel(II) Borate Thin Layer on Ni ₃ B for Efficient Water Oxidation. Angewandte Chemie, 2017, 129, 6672-6677.	1.6	34
339	Discriminating Chiral Molecules of (R)-PPA and (S)-PPA in Aqueous Solution by ECSTM. Angewandte Chemie - International Edition, 2002, 41, 3408-3411.	7.2	33
340	Evidence of a Thermal Annealing Effect on Organic Molecular Assembly. ChemPhysChem, 2003, 4, 857-859.	1.0	33
341	Phase transition of thiophene molecules on Au(111) in solution. Surface Science, 2003, 531, L363-L368.	0.8	33
342	Solutionâ€Crystallized Organic Semiconductors with High Carrier Mobility and Air Stability. Advanced Materials, 2012, 24, 5576-5580.	11.1	33

#	Article	IF	CITATIONS
343	Pd-induced Pt(iv) reduction to form Pd@Pt/CNT core@shell catalyst for a more complete oxygen reduction. Journal of Materials Chemistry A, 2013, 1, 14443.	5.2	33
344	Photoinduced organic nanowires from self-assembled monolayers. Journal of Vacuum Science & Technology an Official Journal of the American Vacuum Society B, Microelectronics Processing and Phenomena, 2002, 20, 2466.	1.6	32
345	A triphenylene-containing side chain liquid crystalline ladder-like polysiloxane and its highly ordered superstructure. Liquid Crystals, 2003, 30, 391-397.	0.9	32
346	STM Investigation of the Photoisomerization of an Azobis-(benzo-15-crown-5) Molecule and Its Self-assembly on Au(111). Journal of Physical Chemistry B, 2006, 110, 3185-3188.	1.2	32
347	Mutual Responsive Hydrazideâ€Based Lowâ€Molecularâ€Mass Organic Gelators: Probing Gelation on the Molecular Level. Chemistry - A European Journal, 2008, 14, 5742-5746.	1.7	32
348	Structural transition of molecular assembly under photo-irradiation: an STM study. Physical Chemistry Chemical Physics, 2008, 10, 6467.	1.3	32
349	Phage M13KO7 detection with biosensor based on imaging ellipsometry and AFM microscopic confirmation. Virus Research, 2009, 140, 79-84.	1.1	32
350	SnO2 hollow spheres: Polymer bead-templated hydrothermal synthesis and their electrochemical properties for lithium storage. Science China Chemistry, 2012, 55, 1314-1318.	4.2	32
351	Synthesis of Benzotrifuran and Benzotripyrrole Derivatives and Molecular Orientations on the Surface and in the Solid State. Chemistry - an Asian Journal, 2013, 8, 2377-2382.	1.7	32
352	Molecular evidence for the intermolecular S⋯S interaction in the surface molecular packing motifs of a fused thiophene derivative. Chemical Communications, 2013, 49, 1829.	2.2	32
353	Redistribution of Li-ions using covalent organic frameworks towards dendrite-free lithium anodes: a mechanism based on a Galton Board. Science China Chemistry, 2020, 63, 1306-1314.	4.2	32
354	Molecular Symmetry Breaking and Chiral Expression of Discotic Liquid Crystals in Two-Dimensional Systems. Journal of Physical Chemistry B, 2002, 106, 13262-13267.	1.2	31
355	Adlayers of Benzotriazole on Cu(110), (100), and (111) in HClO[sub 4] Solution. Journal of the Electrochemical Society, 2002, 149, E367.	1.3	31
356	Site Selective Adsorption and Templated Assembling:  Effects of Organicâ~'Organic Heterogeneous Interface Studied by Scanning Tunneling Microscopy. Journal of Physical Chemistry B, 2004, 108, 1173-1175.	1.2	30
357	Study of fibrinogen adsorption on self-assembled monolayers on Au(111) by atomic force microscopy. Ultramicroscopy, 2005, 105, 129-136.	0.8	30
358	Molecular engineering of Schiff-base linked covalent polymers with diverse topologies by gas-solid interface reaction. Journal of Chemical Physics, 2015, 142, 101905.	1.2	30
359	On-Surface Growth of Single-Layered Homochiral 2D Covalent Organic Frameworks by Steric Hindrance Strategy. Journal of the American Chemical Society, 2020, 142, 14350-14356.	6.6	30
360	In-situ nanoscale insights into the evolution of solid electrolyte interphase shells: revealing interfacial degradation in lithium metal batteries. Science China Chemistry, 2021, 64, 734-738.	4.2	30

#	Article	IF	CITATIONS
361	Layered oxides with solid-solution reaction for high voltage potassium-ion batteries cathode. Chemical Engineering Journal, 2021, 412, 128735.	6.6	30
362	Interfacial Evolution of the Solid Electrolyte Interphase and Lithium Deposition in Graphdiyne-Based Lithium-Ion Batteries. Journal of the American Chemical Society, 2022, 144, 9354-9362.	6.6	30
363	Molecular Organization of Alkoxy-Substituted Oligo(phenylene-ethynylene)s Studied by Scanning Tunneling Microscopy. Langmuir, 2003, 19, 10128-10131.	1.6	29
364	Novel electrocatalytic activity in layered Ni–Cu nanowire arrays. Chemical Communications, 2003, , 3022-3023.	2.2	29
365	Molecular Architecture of Oligothiophene on a Highly Oriented Pyrolytic Graphite Surface by Employing Hydrogen Bondings. Journal of Physical Chemistry B, 2006, 110, 17043-17049.	1.2	29
366	Formation and structural transition of molecular self-assembly on solid surface investigated by scanning tunneling microscopy. Materials Science and Engineering Reports, 2010, 70, 169-187.	14.8	29
367	Controllable synthesis of carbon encapsulated iron phosphide nanoparticles for the chemoselective hydrogenation of aromatic nitroarenes to anilines. Inorganic Chemistry Frontiers, 2018, 5, 1094-1099.	3.0	29
368	Studies of the effects of hydrogen bonding on monolayer structures of C18H37X (X=OH, SH) on HOPG. Chemical Physics Letters, 2001, 348, 321-328.	1.2	28
369	Template-Free Synthesis and Supercapacitance Performance of a Hierachically Porous Oxygen-Enriched Carbon Material. Journal of Nanoscience and Nanotechnology, 2011, 11, 1897-1904.	0.9	28
370	Engineering self-assembled N-doped graphene–carbon nanotube composites towards efficient oxygen reduction electrocatalysts. Physical Chemistry Chemical Physics, 2014, 16, 13605-13609.	1.3	28
371	Controllable atmospheric pressure growth of mono-layer, bi-layer and tri-layer graphene. Chemical Communications, 2014, 50, 11012-11015.	2.2	28
372	Construction of uniform transition-metal phosphate nanoshells and their potential for improving Li-ion battery performance. Journal of Materials Chemistry A, 2018, 6, 8992-8999.	5.2	28
373	Hetero-coupling of a carbonate hydroxide and sulfide for efficient and robust water oxidation. Journal of Materials Chemistry A, 2019, 7, 21959-21965.	5.2	28
374	Adsorption Mode of Cinchonidine on Cu(111) Surface. Journal of the American Chemical Society, 2002, 124, 14300-14301.	6.6	27
375	Structure and Dynamic Process of Two-Dimensional Monodendron Assembly. Chemistry of Materials, 2003, 15, 3098-3104.	3.2	27
376	Electrochemical behavior of multi-wall carbon nanotubes and electrocatalysis of toluene-filled nanotube film on gold electrode. Electrochimica Acta, 2004, 49, 715-719.	2.6	27
377	Enhanced stability and activity with Pd–O junction formation and electronic structure modification of palladium nanoparticles supported on exfoliated montmorillonite for the oxygen reduction reaction. Chemical Communications, 2014, 50, 6660.	2.2	27
378	Remote Chiral Communication in Coadsorberâ€Induced Enantioselective 2D Supramolecular Assembly at a Liquid/Solid Interface. Angewandte Chemie - International Edition, 2015, 54, 4309-4314.	7.2	27

#	Article	IF	CITATIONS
379	Directed block copolymer self-assembly implemented via surface-embedded electrets. Nature Communications, 2016, 7, 10752.	5.8	27
380	Recent progress in the application of in situ atomic force microscopy for rechargeable batteries. Current Opinion in Electrochemistry, 2019, 17, 134-142.	2.5	27
381	Elucidating the interfacial evolution and anisotropic dynamics on silicon anodes in lithium-ion batteries. Nano Energy, 2019, 61, 304-310.	8.2	27
382	Adlayer structures of pyrene and perylene on Cu(111): an in situ STM study. Surface Science, 2001, 478, L320-L326.	0.8	26
383	AFM characterization of gramicidin-A in tethered lipid membrane on silicon surface. Chemical Physics Letters, 2006, 429, 244-249.	1.2	26
384	A simple method to synthesize layered double hydroxide nanoscrolls. Materials Research Bulletin, 2007, 42, 571-575.	2.7	26
385	Effect of Polycyclic Aromatic Hydrocarbons on Detection Sensitivity of Ultratrace Nitroaromatic Compounds. Analytical Chemistry, 2007, 79, 2179-2183.	3.2	26
386	Adaptive Reorganization of 2D Molecular Nanoporous Network Induced by Coadsorbed Guest Molecule. Langmuir, 2014, 30, 3034-3040.	1.6	26
387	Kinetically controlled formation of uniform FePO4 shells and their potential for use in high-performance sodium ion batteries. NPG Asia Materials, 2017, 9, e414-e414.	3.8	26
388	Enabling a Durable Electrochemical Interface via an Artificial Amorphous Cathode Electrolyte Interphase for Hybrid Solid/Liquid Lithiumâ€Metal Batteries. Angewandte Chemie, 2020, 132, 6647-6651.	1.6	26
389	Direct Observation of the Ordering and Molecular Folding of Poly[(m-phenylenevinylene)-co-(2,5-dioctoxy-p-phenylenevinylene)]. Advanced Materials, 2004, 16, 828-831.	11.1	25
390	Metal Octaethylporphyrin Nanowire Array and Network toward Electric/Photoelectric Devices. Journal of Physical Chemistry C, 2009, 113, 16259-16265.	1.5	25
391	Optimizing LiFePO ₄ @C Core–Shell Structures via the 3-Aminophenol–Formaldehyde Polymerization for Improved Battery Performance. ACS Applied Materials & Interfaces, 2014, 6, 22719-22725.	4.0	25
392	Sulfur Confined in Subâ€Nanometerâ€Sized 2 D Graphene Interlayers and Its Electrochemical Behavior in Lithium–Sulfur Batteries. Chemistry - an Asian Journal, 2016, 11, 2690-2694.	1.7	25
393	Template synthesis of imine-based covalent organic framework core-shell structure and hollow sphere: a case of COFTTA-DHTA. Science China Chemistry, 2017, 60, 1098-1102.	4.2	25
394	A Twoâ€Dimensional Holeâ€Transporting Material for Highâ€Performance Perovskite Solar Cells with 20 % Average Efficiency. Angewandte Chemie, 2018, 130, 11125-11131.	1.6	25
395	Hollow carbon nanospheres: syntheses and applications for post lithium-ion batteries. Materials Chemistry Frontiers, 2020, 4, 2283-2306.	3.2	25
396	In Situ STM Evidence for Adsorption of Rhodamine B in Solution. Journal of Physical Chemistry B, 2002, 106, 4223-4226.	1.2	24

#	Article	IF	CITATIONS
397	Self-organized arrays of calix[4]arene and calix[4]arene diquinone disulfide on Au(111). Chemical Physics Letters, 2002, 359, 83-88.	1.2	24
398	Adsorption and Coordination of Tartaric Acid Enantiomers on Cu(111) in Aqueous Solution. Langmuir, 2004, 20, 7360-7364.	1.6	24
399	Engineering the Interfaces of ITO@Cu ₂ S Nanowire Arrays toward Efficient and Stable Counter Electrodes for Quantum-Dot-Sensitized Solar Cells. ACS Applied Materials & Interfaces, 2014, 6, 15448-15455.	4.0	24
400	Unexpected functions of oxygen in a chemical vapor deposition atmosphere to regulate graphene growth modes. Chemical Communications, 2015, 51, 15486-15489.	2.2	24
401	Adlayer Structures of Benzene and Pyridine Molecules on Cu(100) in Solution by ECSTM. Journal of Physical Chemistry B, 2001, 105, 8399-8402.	1.2	23
402	Adlayer Structures of Pyridine, Pyrazine and Triazine on Cu(111):Â an in Situ Scanning Tunneling Microscopy Study. Langmuir, 2002, 18, 5133-5138.	1.6	23
403	The Effect of Polarity on Coadsorbed Molecular Nanostructures of Substituted Phthalocyanine and Thiol Molecules. ChemPhysChem, 2005, 6, 65-70.	1.0	23
404	Nanoarchitectured metal film electrodes with high electroactive surface areas. Thin Solid Films, 2005, 484, 341-345.	0.8	23
405	Quadruply Hydrogen-Bonded Building Block from Hydrazideâ^'Quinolinone Motif and Gelation Ability of Its Analogous Oxalic Monoesterâ ^{~'} Monoamide Derivative. Organic Letters, 2007, 9, 4991-4994.	2.4	23
406	Direct Evidence of Arsenic(III)â^'Carbonate Complexes Obtained Using Electrochemical Scanning Tunneling Microscopy. Analytical Chemistry, 2007, 79, 3615-3622.	3.2	23
407	Effect of the Bridge Alkylene Chain on Adlayer Structure and Property of Functional Oligothiophenes Studied with Scanning Tunneling Microscopy and Spectroscopy. ACS Nano, 2008, 2, 743-749.	7.3	23
408	Two-dimensional OPV4 self-assembly and its coadsorption with alkyl bromide: from helix to lamellar. Chemical Communications, 2009, , 3765.	2.2	23
409	Au–Cu alloy bridged synthesis and optoelectronic properties of Au@CuInSe ₂ core–shell hybrid nanostructures. Journal of Materials Chemistry, 2012, 22, 1765-1769.	6.7	23
410	Dynamic Visualization of Cathode/Electrolyte Evolution in Quasiâ€Solidâ€State Lithium Batteries. Advanced Energy Materials, 2020, 10, 2000465.	10.2	23
411	STM and XRD studies of the adsorption and assembling structures of phthalocyanine and porphyrin. Surface and Interface Analysis, 2002, 34, 767-771.	0.8	22
412	Identification of the Preferential-Bonding Effect of Disubstituted Alkane Derivatives Using Scanning Tunneling Microscopy. Journal of Physical Chemistry B, 2004, 108, 620-624.	1.2	22
413	Two-Dimensional Assemblies of Banana-Shaped Liquid Crystal Molecules on HOPG Surface. Journal of Physical Chemistry B, 2005, 109, 18733-18740.	1.2	22
414	Cobaltâ€Porphyrin atalyzed Oxygen Reduction Reaction: Aâ€Scanning Tunneling Microscopy Study. ChemElectroChem, 2016, 3, 2048-2051.	1.7	22

#	Article	IF	CITATIONS
415	Structurally modulated Li-rich cathode materials through cooperative cation doping and anion hybridization. Science China Chemistry, 2017, 60, 1554-1560.	4.2	22
416	Interface Engineering of a Ceramic Electrolyte by Ta ₂ O ₅ Nanofilms for Ultrastable Lithium Metal Batteries. Advanced Functional Materials, 2022, 32, .	7.8	22
417	Revealing the Correlations between Morphological Evolution and Surface Reactivity of Catalytic Cathodes in Lithium–Oxygen Batteries. Journal of the American Chemical Society, 2021, 143, 21604-21612.	6.6	22
418	Oriented Organic Islands and One-Dimensional Chains on a Au(111) Surface Fabricated by Electrodeposition: An STM Study. Journal of the American Chemical Society, 2008, 130, 12123-12127.	6.6	21
419	La(OH)3 Hollow Nanostructures with Trapezohedron Morphologies Using a New Kirkendall Diffusion Couple. Journal of Physical Chemistry C, 2008, 112, 17988-17993.	1.5	21
420	Synthesis of Wurtzite Cu ₂ ZnGeSe ₄ Nanocrystals and their Thermoelectric Properties. Chemistry - an Asian Journal, 2013, 8, 2383-2387.	1.7	21
421	A Black Phosphorus–Graphite Composite Anode for Liâ€/Naâ€/Kâ€Ion Batteries. Angewandte Chemie, 2020, 13 2338-2342.	³² 1.6	21
422	The Functions and Applications of Fluorinated Interface Engineering in Liâ€Based Secondary Batteries. Small Science, 2021, 1, 2100066.	5.8	21
423	Configurations of a Calix[8]arene and a C60/Calix[8]arene Complex on a Au(111) Surface. Angewandte Chemie, 2003, 115, 2853-2857.	1.6	20
424	Adsorption of Enantiomeric and Racemic Tyrosine on Cu(111):Â A Scanning Tunneling Microscopy Study. Langmuir, 2003, 19, 1958-1962.	1.6	20
425	In Situ STM Evidence for the Adsorption Geometry of Three N-Heteroaromatic Thiols on Au(111). Langmuir, 2011, 27, 7614-7619.	1.6	20
426	Progress of nanoscience in China. Frontiers of Physics, 2014, 9, 257-288.	2.4	20
427	Facile synthesis of hollow Ti2Nb10O29 microspheres for high-rate anode of Li-ion batteries. Science China Chemistry, 2018, 61, 670-676.	4.2	20
428	Effect of Chemically Modified Tips on STM Imaging of 1-Octadecanethiol Molecule. Journal of Physical Chemistry B, 2001, 105, 10465-10467.	1.2	19
429	Catalytic Synthesis and Structural Characterizations of a Highly Crystalline Polyphenylacetylene Nanobelt Array. Journal of the American Chemical Society, 2007, 129, 12922-12923.	6.6	19
430	Detection of VOCs and their concentrations by a single SnO2 sensor using kinetic information. Sensors and Actuators B: Chemical, 2007, 123, 454-460.	4.0	19
431	Hierarchical self-assembly of p-terphenyl derivative with dumbbell-like amphiphilic and rod-coil characteristics. Tetrahedron Letters, 2008, 49, 5522-5526.	0.7	19
432	Electrospray soft-landing for the construction of non-covalent molecular nanostructures using charged droplets under ambient conditions. Chemical Communications, 2016, 52, 13660-13663.	2.2	19

#	Article	IF	CITATIONS
433	Fabrication of bilayer tetrathiafulvalene integrated surface covalent organic frameworks. Physical Chemistry Chemical Physics, 2016, 18, 17356-17359.	1.3	19
434	Highly Orderedp-Xylene Adlayer Formed on Rh(111) in HF Solution:Â In Situ STM and Ex Situ LEED. Langmuir, 2000, 16, 9368-9373.	1.6	18
435	Preparation and dispersion of Ni–Cu composite nanoparticles. Physical Chemistry Chemical Physics, 2002, 4, 3422-3424.	1.3	18
436	Atomic structures of adsorbed sulfur on Cu() in perchloric acid solution by in situ ECSTM. Surface Science, 2002, 499, L159-L163.	0.8	18
437	Effect of Câ [°] 'H···F and Oâ [°] 'H···O Hydrogen Bonding in Forming Self-Assembled Monolayers of BF2-Substituted β-Dicarbonyl Derivatives on HOPG:  STM Investigation. Journal of Physical Chemistry C, 2007, 111, 13851-13854.	1.5	18
438	In Situ Scanning Tunneling Microscopy of Solvent-Dependent Chiral Patterns of 1,4-Di[4- <i>N</i> -(trihydroxymethyl)methyl carbamoylphenyl]-2,5-didodecyloxybenzene Molecular Assembly at a Liquid/Highly Oriented Pyrolytic Graphite Interface. Journal of Physical Chemistry C, 2010, 114, 533-538.	1.5	18
439	Oneâ€Nanometerâ€Precision Control of Al ₂ O ₃ Nanoshells through a Solutionâ€Based Synthesis Route. Angewandte Chemie, 2014, 126, 12990-12994.	1.6	18
440	Controlled formation of core–shell structures with uniform AlPO ₄ nanoshells. Chemical Communications, 2015, 51, 2943-2945.	2.2	18
441	Regulating the charge diffusion of two-dimensional cobalt–iron hydroxide/graphene composites for high-rate water oxidation. Journal of Materials Chemistry A, 2020, 8, 11573-11581.	5.2	18
442	Highly ordered adlayers of three calix[4]arene derivatives on Au(111) surface in HClO4 solution: in situ STM study. Chemical Physics Letters, 2003, 367, 711-716.	1.2	17
443	Adlayer Structures of Calixarenes on Au(111) Surface Studied with STM. Journal of Physical Chemistry B, 2003, 107, 13111-13116.	1.2	17
444	Effect of Chemical Structure on the Adsorption of Amino Acids with Aliphatic and Aromatic Substitution Groups:Â In Situ STM Study. Journal of Physical Chemistry B, 2003, 107, 8474-8478.	1.2	17
445	Organic light-emitting diodes with improved hole-electron balance by using molecular layers of phthalocyanine to modify the anode surface. Applied Physics A: Materials Science and Processing, 2004, 78, 553-556.	1.1	17
446	Bis(ethylenedithio)tetrathiafulvalene Charge-Transfer Salt Nanotube Arrays. Advanced Materials, 2006, 18, 2753-2757.	11.1	17
447	Synthesis, Self-Assembly and Solution-Processed Field-Effect Transistors of a Liquid Crystalline Bis(dithienothiophene) Derivative. Journal of Physical Chemistry C, 2009, 113, 16232-16237.	1.5	17
448	Structural Motif Modulation in 2D Supramolecular Assemblies of Molecular Dipolar Unit Tethered by Alkylene Spacer. Journal of Physical Chemistry C, 2013, 117, 16392-16396.	1.5	17
449	Surface Tectonics of Nanoporous Networks of Melamineâ€Capped Molecular Building Blocks formed through Interface Schiffâ€Base Reactions. Chemistry - an Asian Journal, 2013, 8, 2466-2470.	1.7	17
450	Controlled formation of uniform CeO ₂ nanoshells in a buffer solution. Chemical Communications, 2016, 52, 1420-1423.	2.2	17

#	Article	IF	CITATIONS
451	The intramolecular H-bonding effect on the growth and stability of Schiff-base surface covalent organic frameworks. Physical Chemistry Chemical Physics, 2017, 19, 539-543.	1.3	17
452	In Situ Realization of Waterâ€Mediated Interfacial Processes at Nanoscale in Aprotic Li–O ₂ Batteries. Advanced Energy Materials, 2020, 10, 2002339.	10.2	17
453	Insights into evolution processes and degradation mechanisms of anion-tunable interfacial stability in all-solid-state lithium-sulfur batteries. Energy Storage Materials, 2021, 41, 642-649.	9.5	17
454	Selective Adsorption of Copper Phthalocyanine Atop Functionalized Organic Monolayers. Journal of Physical Chemistry B, 2004, 108, 224-227.	1.2	16
455	Green Production of Ultrahigh-Basicity Polyaluminum Salts with Maximum Atomic Economy by Ultrafiltration and Electrodialysis with Bipolar Membranes. Industrial & Engineering Chemistry Research, 2014, 53, 13467-13474.	1.8	16
456	Direct Probing of the Structure and Electron Transfer of Fullerene/Ferrocene Hybrid on Au(111) Electrodes by in Situ Electrochemical STM. Journal of the American Chemical Society, 2014, 136, 3184-3191.	6.6	16
457	Surface Host–Guest Supramolecular Assemblies on Porphyrin-Based Covalent Organic Grids. Journal of Physical Chemistry C, 2016, 120, 15753-15757.	1.5	16
458	Controlled formation of uniform nanoshells of manganese oxide and their potential in lithium ion batteries. Chemical Communications, 2017, 53, 2846-2849.	2.2	16
459	Competitive chiral induction in a 2D molecular assembly: Intrinsic chirality versus coadsorber-induced chirality. Science Advances, 2017, 3, e1701208.	4.7	16
460	Construction of Uniform Cobalt-Based Nanoshells and Its Potential for Improving Li-Ion Battery Performance. ACS Applied Materials & amp; Interfaces, 2018, 10, 22896-22901.	4.0	16
461	High-Performance Cathode of Sodium-Ion Batteries Enabled by a Potassium-Containing Framework of K _{0.5} Mn _{0.7} Fe _{0.2} Ti _{0.1} O ₂ . ACS Applied Materials & Interfaces, 2020, 12, 15313-15319.	4.0	16
462	Structural Restoration of Degraded LiFePO ₄ Cathode with Enhanced Kinetics Using Residual Lithium in Spent Graphite Anodes. CCS Chemistry, 2023, 5, 1189-1201.	4.6	16
463	Molecule rectifier fabricated by capillary tunnel junction. Chemical Physics Letters, 2002, 361, 465-468.	1.2	15
464	Fabrication, characterization and electrochemical behaviors of the orientated film of a C60 derivative. Surface Science, 2003, 536, L408-L414.	0.8	15
465	The Preparation and in Situ Scanning Tunneling Microscopy Study of Fe(110) Surface. Langmuir, 2003, 19, 1954-1957.	1.6	15
466	Linear dislocation tunes chirality: STM study of chiral transition and amplification in a molecular assembly on an HOPG surface. Chemical Communications, 2009, , 2649.	2.2	15
467	Substituent-Dependent Ordering of Adlayer Structures of Fullerene Derivatives Adsorbed on Au(111): A Scanning Tunneling Microscopy Study. Journal of Physical Chemistry C, 2010, 114, 3170-3174.	1.5	15
468	A novel amphipathic block copolymer coating forming micelle-like aggregates for separation of steroids in open tubular capillary electrochromatography. Talanta, 2011, 84, 501-507.	2.9	15

#	Article	IF	CITATIONS
469	Rechargeable Aluminium–Sulfur Battery with Improved Electrochemical Performance by Cobaltâ€Containing Electrocatalyst. Angewandte Chemie, 2020, 132, 23163-23167.	1.6	15
470	Hydrolysis of Corncob Hemicellulose by Solid Acid Sulfated Zirconia and Its Evaluation in Xylitol Production. Applied Biochemistry and Biotechnology, 2021, 193, 205-217.	1.4	15
471	In situ scanning tunneling microscopy study of adsorption of diaza-15-crown-5 on Cu(111). Surface Science, 2001, 489, L568-L572.	0.8	14
472	Self-assembled monolayer of a Schiff base on Au(111) surface: electrochemistry and electrochemical STM study. Electrochimica Acta, 2002, 48, 303-309.	2.6	14
473	Assembling Nanometer Nickel Particles into Ordered Arrays. ChemPhysChem, 2003, 4, 1114-1117.	1.0	14
474	Surface morphology and nodule formation mechanism of cellulose acetate membranes by atomic force microscopy. Journal of Applied Polymer Science, 2003, 88, 1328-1335.	1.3	14
475	Site-Selective Adsorption of Benzoic Acid Using an Assembly of Tridodecylamine as the Molecular Template. Langmuir, 2003, 19, 9759-9763.	1.6	14
476	Voltage-Dependent Scanning Tunneling Microscopy Images of a Copper Complex on Graphite. Journal of Physical Chemistry B, 2003, 107, 13384-13388.	1.2	14
477	Stacking Phenomenon of Self-assembled Monolayers and Bilayers of Thioalkyl-substituted Tetrathiafulvalene. Chemistry Letters, 2003, 32, 856-857.	0.7	14
478	Dimerization of three xanthene dyes on Au(111) surface. Surface Science, 2004, 551, 204-212.	0.8	14
479	Potential Dependent Adsorption Geometry of 2,5-Dihydroxybenzoic Acid on a Au(111) Surface: An in Situ Electrochemical Scanning Tunneling Microscopy Study. Journal of Physical Chemistry C, 2012, 116, 6208-6214.	1.5	14
480	Switching the surface homochiral assembly by surface host–guest chemistry. Chemical Communications, 2017, 53, 11095-11098.	2.2	14
481	Formation of Porous Films and Vesicular Fibers via Self-Organization of an Amphiphilic Chiral Oligomer. Langmuir, 2004, 20, 2515-2518.	1.6	13
482	Hydrogen Bond Partner Reorganization in the Coadsorption of a Monodendron and Pyridylethynyl Derivatives. Langmuir, 2011, 27, 1292-1297.	1.6	13
483	Donor/acceptor complex of triphenylene and trinitrotoluene on Au(111): a scanning tunneling microscopy study. Chemical Communications, 2011, 47, 6915.	2.2	13
484	Spherical Mesoporous Metal Oxides with Tunable Orientation Enabled by Growth Kinetics Control. Journal of the American Chemical Society, 2020, 142, 17897-17902.	6.6	13
485	Photodimerization of P2VB on Au(111) in Solution Studied with Scanning Tunneling Microscopy. Journal of Physical Chemistry B, 2003, 107, 5116-5119.	1.2	12
486	Programmed Fabrication of Bimetallic Nanobarcodes for Miniature Multiplexing Bioanalysis. Analytical Chemistry, 2009, 81, 2815-2818.	3.2	12

#	Article	IF	CITATIONS
487	Facile Synthesis of <scp>Mo₂C</scp> Nanocrystals Embedded in Nanoporous Carbon Network for Efficient Hydrogen Evolution. Chinese Journal of Chemistry, 2017, 35, 911-917.	2.6	12
488	Potential- and concentration-dependent self-assembly structures at solid/liquid interfaces. Nanoscale, 2018, 10, 3438-3443.	2.8	12
489	Adlayer structure of 1-C18H37 SH molecules: scanning tunnelling microscopy study. Surface and Interface Analysis, 2001, 32, 256-261.	0.8	11
490	A Dimeric Structure of BacteriochlorophyllidecMolecules Studied by Scanning Tunneling Microscopy. Journal of Physical Chemistry B, 2002, 106, 3037-3040.	1.2	11
491	Direct STM Investigation of Cinchona Alkaloid Adsorption on Cu(111). Langmuir, 2004, 20, 3006-3010.	1.6	11
492	TNT adsorption on Au(111): electrochemistry and adlayer structure. Chemical Communications, 2008, , 1877.	2.2	11
493	Synthesis of Nanostructured SnO2/C Microfibers with Improved Performances as Anode Material for Li-Ion Batteries. Journal of Nanoscience and Nanotechnology, 2012, 12, 2581-2585.	0.9	11
494	Block copolymer-templated chemical nanopatterning on pyrolyzed photoresist carbon films. Chemical Communications, 2012, 48, 9741.	2.2	11
495	Solution Effect on Diazonium-Modified Au(111): Reactions and Structures. Langmuir, 2013, 29, 2955-2960.	1.6	11
496	Two-dimensional self-assemblies of telechelic organic compounds: structure and surface host–guest chemistry. Philosophical Transactions Series A, Mathematical, Physical, and Engineering Sciences, 2013, 371, 20120302.	1.6	11
497	Molecular Conductance through a Quadrupleâ€Hydrogenâ€Bondâ€Bridged Supramolecular Junction. Angewandte Chemie, 2016, 128, 12581-12585.	1.6	11
498	Enantiomeric Excess-Tuned 2D Structural Transition: From Heterochiral to Homochiral Supramolecular Assemblies. Langmuir, 2016, 32, 6830-6835.	1.6	11
499	Insights into the nitride-regulated processes at the electrolyte/electrode interface in quasi-solid-state lithium metal batteries. Journal of Energy Chemistry, 2022, 67, 780-786.	7.1	11
500	Anion Doping for Layered Oxides with a Solid-Solution Reaction for Potassium-Ion Battery Cathodes. ACS Applied Materials & Interfaces, 2022, 14, 13379-13387.	4.0	11
501	Scanning Tunneling Microscopy Characterization of Aromatic Molecules Stabilized by a Buffer Layer of Alkane Derivatives. Japanese Journal of Applied Physics, 2001, 40, 4273-4276.	0.8	10
502	In situ electrochemical STM of charge-transfer complex on Cu(). Surface Science, 2002, 517, 52-58.	0.8	10
503	Stacking behavior of 2-D assemblies of octa-alkoxyl-substituted phthalocyanine studied by scanning tunneling microscopy. Surface Science, 2004, 559, 40-46.	0.8	10
504	The effects of annealing on the structures and electrical conductivities of fullerene-derived nanowires. Journal of Materials Chemistry, 2004, 14, 914.	6.7	10

#	Article	IF	CITATIONS
505	Adsorption of TTF, TCNQ and TTF-TCNQ on Au(111): An in situ ECSTM study. Science in China Series B: Chemistry, 2009, 52, 559-565.	0.8	10
506	Turning off the majority-rules effect in two-dimensional hierarchical chiral assembly by introducing a chiral mismatch. Nanoscale, 2016, 8, 17861-17868.	2.8	10
507	Insight into the Interfacial Process and Mechanism in Lithium–Sulfur Batteries: An In Situ AFM Study. Angewandte Chemie, 2016, 128, 16067-16071.	1.6	10
508	Molecular Quadripod as a Noncovalent Interfacial Coupling Reagent for Forming Immobilized Coordination Assemblies. Journal of the American Chemical Society, 2018, 140, 12337-12340.	6.6	10
509	Tri-Stable Structural Switching in 2D Molecular Assembly at the Liquid/Solid Interface Triggered by External Electric Field. ACS Nano, 2019, 13, 6751-6759.	7.3	10
510	Absolute Configuration of Monodentate Phosphine Ligand Enantiomers on Cu(111). Analytical Chemistry, 2004, 76, 627-631.	3.2	9
511	STM Investigation of Substitute Effect on Oligothiophene Adlayer at Au(111) Substrate. Journal of Nanoscience and Nanotechnology, 2007, 7, 3111-3116.	0.9	9
512	Shapeâ€Persistent Two omponent 2 D Networks with Atomicâ€Size Tunability. Chemistry - an Asian Jourr 2011, 6, 2426-2430.	ıal 1.7	9
513	Cost-Effective Production of Pure Al13 from AlCl3 by Electrolysis. Industrial & Engineering Chemistry Research, 2012, 51, 11201-11206.	1.8	9
514	In Situ Scanning Tunneling Microscopy Investigation of Subphthalocyanine and Subnaphthalocyanine Adlayers on a Au(111) Electrode. Langmuir, 2013, 29, 264-270.	1.6	9
515	Electrostatic-Interaction-Induced Molecular Deposition of a Hybrid Bilayer on Au(111): A Scanning Tunneling Microscopy Study. Langmuir, 2014, 30, 3502-3506.	1.6	9
516	Controlled synthesis of hierarchically-structured MnCo2O4 and its potential as a high performance anode material. Science China Chemistry, 2017, 60, 1180-1186.	4.2	9
517	Crystallization-induced self-hollowing of molybdenum sulfide nanoparticles and their potential in sodium ion batteries. Chemical Communications, 2019, 55, 5894-5897.	2.2	9
518	Adlayer structure of TCNQ molecules on Cu(111): Anin situ STM study. Science Bulletin, 2001, 46, 377-379.	1.7	8
519	In situ STM of phenolic compounds on Cu() in solution. Surface Science, 2002, 520, L625-L632.	0.8	8
520	Langmuir film behaviors of dendrons at water–air interface. Chemical Physics Letters, 2003, 370, 542-547.	1.2	8
521	Tuning molecular orientation with STM at the solid/liquid interfaceElectronic supplementary information (ESI) available: chemical structures of triptycene and triphenylene molecules and STM image of triphenylene molecules on Cu(111). See http://www.rsc.org/suppdata/cc/b3/b308155a/. Chemical Communications, 2003, 2874.	2.2	8
522	Self-organization of surfactant molecules on solid surface: an STM study of sodium alkyl sulfonates. Applied Surface Science, 2005, 240, 13-18.	3.1	8

#	Article	IF	CITATIONS
523	Adlayer Structures of Aza- and/or Oxo-Bridged Calix[2]arene[2]triazines on Au(111) Investigated by Scanning Tunneling Microscopy (STM). Langmuir, 2007, 23, 8021-8027.	1.6	8
524	The structural details and substituent effects on biphenyls adlayers with halogen/pseudohalogen substituents on Au(111): An STM investigation. Journal of Electroanalytical Chemistry, 2013, 688, 237-242.	1.9	8
525	Hybrid molecular nanostructures with donor-acceptor chains. Science China Chemistry, 2013, 56, 124-130.	4.2	8
526	lonic interaction-induced assemblies of bimolecular "chessboard―structures. Chemical Communications, 2017, 53, 9129-9132.	2.2	8
527	Charge Rateâ€Dependent Decomposition Mechanism of Toroidal Li 2 O 2 in Liâ€O 2 Batteries. Chinese Journal of Chemistry, 2021, 39, 2668-2672.	2.6	8
528	Structure of thiocyanate adlayers on Rh(111): an in situ STM study. Journal of Solid State Electrochemistry, 1997, 1, 45-52.	1.2	7
529	Adlayer Structures of Organic Molecules with Different Functional Groups on Cu(111) in Solution. Journal of Physical Chemistry B, 2002, 106, 11272-11276.	1.2	7
530	Thermally stimulated transition in tunneling characteristics of molecular junction of tin/octadecanol/tin. Chemical Physics Letters, 2003, 380, 767-773.	1.2	7
531	Visible light induced photocatalytic reaction of rhodamine B dye via 12-tungstosilicic acid in water. Science in China Series B: Chemistry, 2003, 46, 577.	0.8	7
532	Electrochemical Construction of Novel C60 Derivative/PPV Composite Adlayer on Cu(111) and Their Current/Voltage Characteristics. Journal of Physical Chemistry B, 2004, 108, 965-970.	1.2	7
533	Monitoring molecular motion and structure near defect with STM. Colloids and Surfaces A: Physicochemical and Engineering Aspects, 2005, 257-258, 9-13.	2.3	7
534	Molecular adlayer and photo-induced structural transformation of a diarylethene derivative on Au(111) investigated with scanning tunneling microscopy. Journal of Electroanalytical Chemistry, 2011, 656, 304-311.	1.9	7
535	Facile Solution Synthesis and Photoelectric Properties of Monolithic Tin(II) Sulfide Nanobelt Arrays. Chemistry - an Asian Journal, 2013, 8, 2483-2488.	1.7	7
536	Conformation Diversity of a Fusedâ€Ring Pyrazine Derivative on Au(111) and Highly Ordered Pyrolytic Graphite. Chemistry - an Asian Journal, 2015, 10, 1311-1317.	1.7	7
537	Manifesting the sergeants-and-soldiers principle in coadsorber induced homochiral polymorphic assemblies at the liquid/solid interface. Chemical Communications, 2016, 52, 12088-12091.	2.2	7
538	Highâ€Temperature Formation of a Functional Film at the Cathode/Electrolyte Interface in Lithium–Sulfur Batteries: An Inâ€Situ AFM Study. Angewandte Chemie, 2017, 129, 14625-14629.	1.6	7
539	Self-supported metal sulphide nanocrystals-assembled nanosheets on carbon paper as efficient counter electrodes for quantum-dot-sensitized solar cells. Science China Chemistry, 2018, 61, 1338-1344.	4.2	7
540	Construction of uniform ZrO ₂ nanoshells by buffer solutions. Dalton Transactions, 2018, 47, 12843-12846.	1.6	7

#	Article	IF	CITATIONS
541	Electrode materials for lithium secondary batteries with high energy densities. Scientia Sinica Chimica, 2011, 41, 1229-1239.	0.2	7
542	Pd Porphyrin Cofacial Dimer Formed via CO2 Binding: An in Situ Electrochemistry Scanning Tunneling Microscopy Study. Journal of Physical Chemistry C, 2021, 125, 24915-24919.	1.5	7
543	Study of β-amyloid adsorption and aggregation on graphite by STM and AFM. Science Bulletin, 2003, 48, 437-440.	1.7	6
544	Nanofrictional Properties of Dendron Langmuir–Blodgett Films. Chemistry Letters, 2003, 32, 290-291.	0.7	6
545	Tunneling Characteristics of Octadecyl Derivatives on Tin and Indium Electrodes. Langmuir, 2004, 20, 855-861.	1.6	6
546	Surface Structure of Heterogeneous Catalysts: Cinchona and Tartaric Acid on Solid Surface. Topics in Catalysis, 2005, 35, 131-139.	1.3	6
547	Dispersion of Metallofullerene Y@C82on Bare, C60-Modified, and Iodine-Modified Au(111) Surfaces Investigated with ECSTM. Journal of Physical Chemistry B, 2006, 110, 5559-5562.	1.2	6
548	Structural Comparison of Self-Organized Adlayers of Ligands and Their Metal-Coordinated Complexes on a Au(111) Surface: An STM Study. Chemistry - A European Journal, 2006, 12, 2808-2814.	1.7	6
549	Bio-active molecule immobilisation on layered double hydroxides. International Journal of Nanotechnology, 2006, 3, 545.	0.1	6
550	2D Hexagonal Tilings Based on Triangular and Hexagonal Structural Units in the Selfâ€Assembly of Thiacalix[4]arene Tetrasulfonate on an Au(111) Surface. Chemistry - an Asian Journal, 2011, 6, 1811-1816.	1.7	6
551	Si@Cu@Au AFM tips for tip-enhanced Raman spectrum. Science China Chemistry, 2015, 58, 1494-1500.	4.2	6
552	Hollowâ€Structured Electrode Materials: Selfâ€Templated Synthesis and Their Potential in Secondary Batteries. ChemNanoMat, 2020, 6, 1298-1314.	1.5	6
553	Inâ€Situ Scanning Tunneling Microscopy of Cobaltâ€Phthalocyanineâ€Catalyzed CO 2 Reduction Reaction. Angewandte Chemie, 2020, 132, 16232-16237.	1.6	6
554	Molecular Linking Stabilizes Bi Nanoparticles for Efficient Electrochemical Carbon Dioxide Reduction. Journal of Physical Chemistry C, 2021, 125, 12699-12706.	1.5	6
555	Precise surface control of cathode materials for stable lithium-ion batteries. Chemical Communications, 2022, 58, 1454-1467.	2.2	6
556	Selective Extraction of Transition Metals from Spent LiNi _{<i>x</i>} Co _y Mn _{1â^<i>x</i>â^²<i>y</i>} O ₂ Cathode via Regulation of Coordination Environment. Angewandte Chemie, 2022, 134, .	1.6	6
557	Discriminating Chiral Molecules of (R)-PPA and (S)-PPA in Aqueous Solution by ECSTM. Angewandte Chemie, 2002, 114, 3558-3561.	1.6	5
558	Controlled assembly of copper phthalocyanine with 1-iodooctadecane. Science Bulletin, 2003, 48, 1519-1524.	1.7	5

#	Article	IF	CITATIONS
559	A dimeric structure of eosin molecules on Au(111) surface. Chemical Physics Letters, 2003, 370, 268-273.	1.2	5
560	Chiral discrimination in Langmuir and Langmuir–Blodgett film of axially chiral 1,1′-binaphthyl acid. Surface Science, 2003, 527, L171-L176.	0.8	5
561	Adlayer structure of 4-ethyl naphthalene-1-sulfonate on Cu. Surface Science, 2003, 531, 226-230.	0.8	5
562	A direct observation on the surface assembling and ordering of coumarin derivatives on the graphite surface. Surface Science, 2004, 559, 70-76.	0.8	5
563	Solid-State Supramolecular Chemistry of Zn-Tetraphenylporphyrins with 4,4-Dipyridyl N,N-Dioxide and Hexamethylenetetramine. Letters in Organic Chemistry, 2005, 2, 424-427.	0.2	5
564	Disorder–Order Transformation of Trithiocyanuric Acid Adlayer on a Au(111) Surface Induced by Electrode Potential. Journal of Physical Chemistry C, 2011, 115, 16583-16589.	1.5	5
565	Scanning Tunneling Microscopy Investigation of Copper Phthalocyanine and Truxenone Derivative Binary Superstructures on Graphite. Chemistry - an Asian Journal, 2011, 6, 424-429.	1.7	5
566	Supercapacitor-battery hybrid energy storage devices from an aqueous nitroxide radical active material. Science Bulletin, 2011, 56, 2433-2436.	1.7	5
567	Monolayer graphene-supported free-standing PS-b-PMMA thin film with perpendicularly orientated microdomains. RSC Advances, 2014, 4, 63941-63945.	1.7	5
568	Electron Transport Characteristics of the Dimeric 1,4â€Benzenedithiol Junction. Chemistry - an Asian Journal, 2014, 9, 2077-2082.	1.7	5
569	Optoeletronic investigation of Cu2ZnSn(S,Se)4 thin-films & Cu2ZnSn(S,Se)4/CdS interface with scanning probe microscopy. Science China Chemistry, 2016, 59, 231-236.	4.2	5
570	Development of simulation approach for two-dimensional chiral molecular self-assembly driven by hydrogen bond at the liquid/solid interface. Surface Science, 2017, 663, 71-80.	0.8	5
571	Directed assembly of fullerene on modified Au(111) electrodes. Chemical Communications, 2018, 54, 8052-8055.	2.2	5
572	Interfacial Evolution of Lithium Dendrites and Their Solid Electrolyte Interphase Shells of Quasiâ€Solidâ€State Lithiumâ€Metal Batteries. Angewandte Chemie, 2020, 132, 18277-18282.	1.6	5
573	Adlayer structure of P2VB on iodine-modified Au(111) in solution. Surface Science, 2002, 511, L298-L302.	0.8	4
574	Two-Component Assembling of Phthalocyanine with Alkane Derivatives on Graphite Surface. Japanese Journal of Applied Physics, 2003, 42, 4729-4733.	0.8	4
575	Delaying photobleaching and recovering luminescence of a DNA molecular light switch in DNA analysis. Analytical Biochemistry, 2004, 329, 334-336.	1.1	4
576	Electrochemical Scanning Tunneling Microscope Imaging of Self-Assembled Monolayer of Double-Stranded DNA on Au(111). Journal of Nanoscience and Nanotechnology, 2004, 4, 561-564.	0.9	4

#	Article	IF	CITATIONS
577	Facile Synthesis of Pt Multipods Nanocrystals. Journal of Nanoscience and Nanotechnology, 2006, 6, 2031-2036.	0.9	4
578	From Amphiphilic Organic Ligands to Metal-Coordinated Complexes:  Structural Difference in Their Self-Organizations Studied by STM. Journal of Physical Chemistry C, 2007, 111, 4667-4672.	1.5	4
579	Substitution effect on the adlayer formation of tetrachloroperylene bisimides on HOPG surface. Surface Science, 2010, 604, 2078-2083.	0.8	4
580	Synthesis of Flake-Like MnO ₂ /CNT Composite Nanotubes and Their Applications in Electrochemical Capacitors. Journal of Nanoscience and Nanotechnology, 2011, 11, 1996-2002.	0.9	4
581	Adlayer structures of thiophene and pyrrole derivatives on Au(1 1 1) probed by scanning tunneling microscopy. Journal of Electroanalytical Chemistry, 2014, 716, 87-92.	1.9	4
582	High-resolution imaging of graphene by tip-enhanced coherent anti-Stokes Raman scattering. Journal of Innovative Optical Health Sciences, 2019, 12, .	0.5	4
583	Direct Visualization of Dynamic Mobility of Li ₂ O ₂ in Li–O ₂ Batteries: A Differential Interference Microscopy Study. ACS Applied Materials & Interfaces, 2022, 14, 5395-5401.	4.0	4
584	Lewis Acid Catalyzed Synthesis of Vinylene Linked Two Dimensional Covalent Organic Frameworks. Chinese Journal of Chemistry, 0, , .	2.6	4
585	In situ scanning tunneling microscopy of maleic acid and fumaric acid adsorbed on Pt(111). Journal of Electroanalytical Chemistry, 2001, 500, 156-162.	1.9	3
586	Effect of alkyl substitutions on self-assembly. Science Bulletin, 2002, 47, 1514.	1.7	3
587	Structure of self-assembled monolayer of NPAN on Au(111) electrode. Science Bulletin, 2003, 48, 1952-1955.	1.7	3
588	Synthesis of a novel axially chiral amphiphile and study on its assembly behavior in two and three dimensionsElectronic supplementary information (ESI) available: experimental details. See http://www.rsc.org/suppdata/cc/b3/b302572a/. Chemical Communications, 2003, , 1498.	2.2	3
589	Adlayer Structures of Binaphthyl Derivatives on Cu(111). Chemistry Letters, 2003, 32, 702-703.	0.7	3
590	Direct Observation of the DNA Multimolecule Condensation with Fluorescence Microscopy. Chemistry Letters, 2003, 32, 80-81.	0.7	3
591	A Simple Route to Platinum and Pt-Based Composite Nanotubes. Journal of Nanoscience and Nanotechnology, 2005, 5, 1929-1932.	0.9	3
592	Topography and functional information of plasma membrane. Science in China Series C: Life Sciences, 2008, 51, 95-103.	1.3	3
593	Macro-micro factors affecting real estate demand analysis. , 2009, , .		3
594	Surface-Confined Conformers and Coassembly-Induced Conformer Resolution. Langmuir, 2011, 27, 9994-9999.	1.6	3

#	Article	IF	CITATIONS
595	MOLECULAR TEMPLATES FOR CONTROLLING AND ORDERING ORGANIC MOLECULES ON SOLID SURFACES. Nano, 2012, 07, 1230001.	0.5	3
596	Carbon-free Cu2ZnSn(S,Se)4 film prepared via a non-hydrazine route. Science China Chemistry, 2014, 57, 1552-1558.	4.2	3
597	A continuous etching process for highly-active Pd nanoclusters and their in situ stabilization. RSC Advances, 2014, 4, 23637.	1.7	3
598	Batteries: A High-Energy Room-Temperature Sodium-Sulfur Battery (Adv. Mater. 8/2014). Advanced Materials, 2014, 26, 1308-1308.	11.1	3
599	<i>In situ</i> AFM Investigation of Interfacial Morphology of Single Crystal Silicon Wafer Anode. Wuli Huaxue Xuebao/ Acta Physico - Chimica Sinica, 2016, 32, 283-289.	2.2	3
600	Self-assembly of a sulfur-bridged annulene: Substrate effect and donor-acceptor complex. Journal of Electroanalytical Chemistry, 2016, 781, 20-23.	1.9	3
601	Self-assembly of an oligo(<i>p</i> -phenylenevinylene)-based molecule on an HOPG surface: insights from multi-scale simulation and STM observation. RSC Advances, 2018, 8, 31868-31873.	1.7	3
602	Chemoselective Onâ€surface Homocoupling of Terminal Alkynes Catalyzed by Exogenous Cupric Ions. Chemistry - an Asian Journal, 2020, 15, 2627-2630.	1.7	3
603	A General Synthesis Strategy for Hollow Metal Oxide Microspheres Enabled by Gelâ€Assisted Precipitation. Angewandte Chemie - International Edition, 2021, 60, 21377-21383.	7.2	3
604	Scanning tunneling microscopy image contrast variation on a copper (II) complex adlayer with tip–sample separation. Surface Science, 2002, 513, L436-L440.	0.8	2
605	STM investigation of surfactant molecules. Science Bulletin, 2002, 47, 894.	1.7	2
606	Fabrication of a thin film containing C 60 derivative nanodomains by photo- polymerization of diacetylene acid. Applied Physics A: Materials Science and Processing, 2003, 77, 757-760.	1.1	2
607	Immune-microassay with optical proteinchip for protein detection. , 0, , .		2
608	Ordered arrays of semi-crown ligands on an Au(111) electrode surface: in situ STM study. Science in China Series B: Chemistry, 2004, 47, 320.	0.8	2
609	Adlayer structures of dl-homocysteine and l-homocysteine thiolactone on Au(1 1 1) surface: an in situ STM study. Electrochimica Acta, 2004, 49, 1629-1633.	2.6	2
610	Fabrication of a composite nano-ultrathin film of poly-phenylene-vinylene and C60 derivative. Colloids and Surfaces A: Physicochemical and Engineering Aspects, 2005, 257-258, 195-198.	2.3	2
611	Investigation of ITO surface modified by NPB and arachidic acid LB films. Colloids and Surfaces A: Physicochemical and Engineering Aspects, 2005, 257-258, 433-437.	2.3	2
612	Theoretical understanding of adlayer structure, thermal stability and electronic property of graphene molecules. Surface Science, 2010, 604, 2091-2097.	0.8	2

#	Article	IF	CITATIONS
613	Formation and Structure of p-Nitrobenzoic Acid Adlayer on Au(111) Surface in HClO ₄ Investigated by <i>In-Situ</i> Scanning Tunneling Microscopy. Journal of Nanoscience and Nanotechnology, 2011, 11, 4800-4805.	0.9	2
614	Formation of host–guest structure at an electrified electrode surface: An electrochemical STM investigation. Electrochemistry Communications, 2012, 17, 82-84.	2.3	2
615	Editorial of the PCCP themed issue "Scanning tunneling microscopy: revealing new physical chemistry insight― Physical Chemistry Chemical Physics, 2013, 15, 12412.	1.3	2
616	The formation of an ordered microporous aluminum-based material mediated by phthalic acid. Chemical Communications, 2016, 52, 8038-8041.	2.2	2
617	Innentitelbild: A Flexible Solid Electrolyte Interphase Layer for Longâ€Life Lithium Metal Anodes (Angew.) Tj ETQq1	1 0.7843 1.6	14 rgBT /○ 2
618	Controlling the reaction kinetics in solution for uniform nanoshells of metal sulfides with sub-nanometer accuracy. Science Bulletin, 2019, 64, 232-235.	4.3	2
619	2020 emerging investigator issue of Science China Chemistry. Science China Chemistry, 2020, 63, 1331-1335.	4.2	2
620	Lattice-confined Ru clusters for hydrogen oxidation reaction with high CO-tolerance. Science China Chemistry, 2020, 63, 1169-1170.	4.2	2
621	Study of β-amyloid adsorption and aggregation on graphite by STM and AFM. Science Bulletin, 2003, 48, 437.	1.7	2
622	The Self-assembly Structure of Pyrazine Derivative on Highly Oriented Pyrolytic Graphite. Wuli Huaxue Xuebao/ Acta Physico - Chimica Sinica, 2005, 21, 925-928.	2.2	2
623	<i>In Situ</i> / <i>Operando</i> Advances of Electrode Processes in Solid-state Lithium Batteries. Acta Chimica Sinica, 2021, 79, 1197.	0.5	2
624	2021 Emerging Investigator Issue of Science China Chemistry. Science China Chemistry, 2021, 64, 1811-1816.	4.2	2
625	Assembling Behavior of BINAP Derivative. Chemistry Letters, 2002, 31, 706-707.	0.7	1
626	Direct observation of monomer film structure of bacteriochlorophyll c. Science Bulletin, 2003, 48, 2307.	1.7	1
627	Ordered Ni—Cu Nanowire Array with Enhanced Coercivity ChemInform, 2003, 34, no.	0.1	1
628	Towards total dissolution of full length unmodified carbon nanotubes (CNT) and its application to fabrication of ultra-thin CNT films at the water/air interface. Journal of Materials Chemistry, 2003, 13, 1244.	6.7	1
629	Evaluation for cell affinity of the composite material containing carbon nanotubes. Science Bulletin, 2004, 49, 2126.	1.7	1
630	Controlled fabrication of fullerene derivative one-dimensional nanostruc-tures via electrophoretic depo-sition of its clusters. Science Bulletin, 2004, 49, 2021.	1.7	1

#	Article	IF	CITATIONS
631	Self-assembled structure of alkyloxy substituted benzoic acid methyl ester on HOPG: An STM study. Science Bulletin, 2004, 49, 2590.	1.7	1
632	Comment on On the Existence of Ordered Organic Adlayers at the Cu(111)/Electrolyte Interface. Langmuir, 2004, 20, 2807-2807.	1.6	1
633	Ordered Self-assembled Monolayers of β-dicarbonyl Derivatives Studied by STM. Acta Physico-chimica Sinica, 2006, 22, 691-695.	0.6	1
634	Self-assembly of 4-(amyloxy) cinnamic acid on HOPG and its photoinduced transformation: An STM study. Science Bulletin, 2006, 51, 1389-1392.	1.7	1
635	STRUCTURES OF Ni(II) OCTAETHYLPORPHYRIN AND C60 AT Au(111) SURFACE INVESTIGATED BY STM. Nano, 2006, 01, 95-100.	0.5	1
636	Discursive imbalance and deficiency in intercultural news communication. Chinese Journal of Communication, 2008, 1, 156-167.	1.3	1
637	Chiral Molecular Cavities of Calix[4]Crown on Au(111). Journal of Nanoscience and Nanotechnology, 2008, 8, 5702-5707.	0.9	1
638	Processes in chemical reactions related to the environment, energy and materials sciences. Physical Chemistry Chemical Physics, 2011, 13, 1923.	1.3	1
639	Organic Semiconductors: Solution rystallized Organic Semiconductors with High Carrier Mobility and Air Stability (Adv. Mater. 41/2012). Advanced Materials, 2012, 24, 5518-5518.	11.1	1
640	Batteries: Encapsulation of Sulfur in a Hollow Porous Carbon Substrate for Superior Liâ€5 Batteries with Long Lifespan (Part. Part. Syst. Charact. 4/2013). Particle and Particle Systems Characterization, 2013, 30, 392-392.	1.2	1
641	Solvent-Assisted Preparation of High-Performance Mesoporous CH3NH3PbI3 Perovskite Solar Cells. Journal of Nanoscience and Nanotechnology, 2016, 16, 844-850.	0.9	1
642	2D Co-crystallization of molecular homologues promoted by size complementarity of the alkyl chains at the liquid/solid interface. Physical Chemistry Chemical Physics, 2019, 21, 17846-17851.	1.3	1
643	Observation of contrast variations of a copper (â¡) complex by scanning tunneling microscopy. Science Bulletin, 2003, 48, 531.	1.7	0
644	2D self-assembling of 4, 5-didodecylthiolphthalonitrile on graphite surface. Science Bulletin, 2003, 48, 742-745.	1.7	0
645	Pt Hollow Nanospheres: Facile Synthesis and Enhanced Electrocatalysts ChemInform, 2004, 35, no.	0.1	0
646	Electronic Characteristics of Au-Mercaptohexadecanoic Acid-Au Junction in a Capillary. Journal of Nanoscience and Nanotechnology, 2004, 4, 1081-1084.	0.9	0
647	Self-Assembled Vanadium Pentoxide (V2O5) Hollow Microspheres from Nanorods and Their Application in Lithium-Ion Batteries ChemInform, 2005, 36, no.	0.1	0
648	Title is missing!. Ultramicroscopy, 2005, 105, vii-viii.	0.8	0

#	Article	IF	CITATIONS
649	2D self-assembly of 1,3,2-dioxaborine derivatives on HOPG. Science Bulletin, 2007, 52, 2486-2490.	1.7	0
650	Materials Science at the Institute of Chemistry, Chinese Academy of Sciences. Advanced Materials, 2008, 20, 2811-2811.	11.1	0
651	Surface host-guest assembly as a bottom-up approach for the construction of functional molecular nanostructures. , 2010, , .		0
652	On-Surface Dynamic Covalent Chemistry. Advances in Atom and Single Molecule Machines, 2016, , 221-235.	0.0	0
653	A General Synthesis Strategy for Hollow Metal Oxide Microspheres Enabled by Gelâ€Assisted Precipitation. Angewandte Chemie, 2021, 133, 21547-21553.	1.6	0
654	2D self-assembling of 4,5-didodecylthiolphthalonitrile ongraphite surface. Science Bulletin, 2003, 48, 742.	1.7	0
655	Adsorption of Aromatic Molecules at Solid/Liquid Interface Investigated by Electrochemical STM. Hyomen Kagaku, 2003, 24, 726-733.	0.0	0
656	Controlled assembly of copper phthalocyanine with 1-iodooctadecane. Science Bulletin, 2003, 48, 1519.	1.7	0
657	Structure of self-assembled monolayer of NPAN on Au(111) electrode. Science Bulletin, 2003, 48, 1952.	1.7	0
658	Nanostructures at Solid/Liquid Interface. , 2003, , 85-92.		0
659	Molecular Nanostructures on Metal Surfaces and Their Properties. Wuli Huaxue Xuebao/ Acta Physico - Chimica Sinica, 2005, 21, 690-696.	2.2	0
660	Fabrication and Manipulation of Molecular Nanostructure with Metal-Coordinated Compound on Solid Surfaces Investigated by STM. Wuli Huaxue Xuebao/ Acta Physico - Chimica Sinica, 2009, 25, 389-400.	2.2	0
661	Fullerene Band-Like Assembly Induced by a Donor- ï€ -Acceptor Molecular Template on Au(111) Electrode Surface. Wuli Huaxue Xuebao/ Acta Physico - Chimica Sinica, 2010, 26, 1893-1897.	2.2	0
662	Hierarchically Nanostructured Electrode Materials for Lithium-Ion Batteries. , 2011, , 237-266.		0